XVIII INTERNATIONAL SIIV SUMMER SCHOOL
Sustainable Pavements and Road Materials
Università degli Studi di Napoli Parthenope
Villa Doria d'Angri, Napoli, September 5th-9th 2022

Reusing jet grouting waste for making road pavements base layers

Prof. Ing. Francesca Russo
Università degli Studi di Napoli Federico II
Ing. Cristina Oreto
Università degli Studi di Napoli Federico II

5-9 SEPTEMBER .22
Università di Napoli Parthenope

TABLE OF CONTENTS

- Innovative Material Reused
- Laboratory investigation
- Life Cycle Assessment (LCA)
- Multi-Criteria decision analysis
- Conclusions

JET GROUTING WASTE

a)¤ b)¤ c)¤

Figure·2·Jet·grouting·waste:·a)·jet·grouting·columns,·b)·JGW·drawn·to·the·surface;·c)·JGW·after·grinding·action¶

JET GROUTING WASTE

a)¤ b)¤ c)¤

Figure·2·Jet·grouting·waste:·a)·jet·grouting·columns,·b)·JGW·drawn·to·the·surface;·c)·JGW·after·grinding·action¶

Jet Grouting Waste (JGW) deriving from soil consolidation activities

Jet grouting technique is based on the injection of grout (water and cement based fluid mixture) into the soil at a very high flow rate (200÷400 L/min), with a very high velocity of energy through small-diameter injection nozzles (1÷10 mm) placed on a grout pipe or rod

The jet grout propagates radially with respect to the treatment axis from the borehole at a constant rate of rotation, separating the soil particles. The particles are then mixed and cemented with the jet grout.

After this, the rod is slowly withdrawn toward the surface forming a homogeneous mass of high-strength soil-cement body (the jet column) due to the solidification of the injected cement-based grout

During soil consolidation works, the waste of jet grout is expelled together with extracted soil that is replaced by the grout column

JET GROUTING WASTE

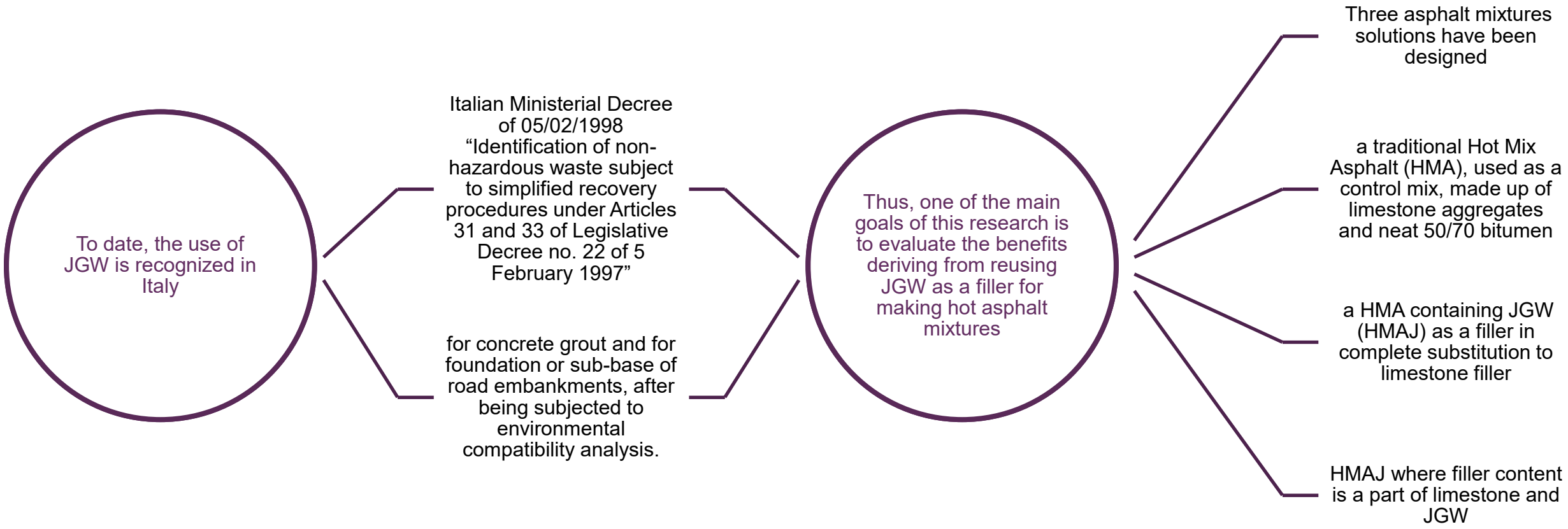

Jet grouting waste

The JGW (see Figures) derived from soil consolidation during underground highway tunnel

it was reused as a filler for designing hot asphalt mixtures after a laboratory grinding process

a ball mill was adopting for 2 hours almost, dried into a oven at 105°C, no weight variation was found in terms of grading size

The main properties investigated of JGW were density (EN 1097-6)  equal to 2.687 g/cm^3 and Rigden voids (EN 1097-4) equal to 53%

Tabella 1 - Requisiti di granulometria per filler addizionato (prospetto 24 della normativa UNI EN 13043)

Dimensione staccio mm	Percentuale passante in massa	
	Intervallo complessivo per i singoli risultati	Intervallo massimo di granulometria dichiarata dal produttore[a)]
2	100	-
0,125	da 85 a 100	10
0,063	da 70 a 100	10

a) Intervallo di granulometria dichiarato sulla base degli ultimi 20 valori (vedere prospetto B.4, riga 1). Il 90% dei risultati dichiarati deve rientrare in questo intervallo, ma tutti i risultati devono rientrare nell'intervallo complessivo di granulometria (vedere colonna 2 sopra).

LIMESTONE AGGREGATES

Coarse and fine limestone aggregates here used for making hot and cold asphalt mixtures were from a quarry located in Southern Italy (Table shows the main features).

Aggregate size	Density	Los Angeles	Shape Index	Flattening Index	Equivalent sand	Rigden voids
	(g/cm^3) EN 1097-6	(%) EN 1097-2	(%) EN 933-4	(%) EN 933-3	(%) EN 933-8	(%) EN 1097-4
Coarse aggregates						
31.5-16mm	2.68	-	4	16	-	-
10-16mm	2.69	16	4	8	-	-
6-12mm	2.71	16.4	8	11	-	-
Fine aggregates						
Sand	2.71	-	-	-	80	-
Filler	2.73	-	-	-	-	46

LIMESTONE AGGREGATES

Coarse and fine limestone aggregates here used for making hot and cold asphalt mixtures were from a quarry located in Southern Italy (Table shows the main features).

Aggregate size	Density	Los Angeles	Shape Index	Flattening Index	Equivalent sand	Rigden voids
	(g/cm^3) EN 1097-6	(%) EN 1097-2	(%) EN 933-4	(%) EN 933-3	(%) EN 933-8	(%) EN 1097-4
Coarse aggregates						
31.5-16mm	2.68	-	4	16	-	-
10-16mm	2.69	16	4	8	-	-
6-12mm	2.71	16.4	8	11	-	-
Fine aggregates						
Sand	2.71	-	-	-	80	-
Filler	2.73	-	-	-	-	46

JGW vs LIMESTONE FILLER: BASE PROPERTIES

Filler type	Specific gravity [g/cm^3] UNI EN 1097-6	Ridgen voids [%] UNI EN 1097-7	Specific surface area [cm^2/g] ISO 9277
Limestone filler	2.737	46	5480
Jet grouting waste	2.687	53	5970

CHEMICAL COMPOSITION of JGW and LEACHING TEST

JGW Chemical composition

The samples of grided JTW were prepared in compliance with UNI 10802:2013.

Each sample was dried to minimize losses due to adhesion between the material and the equipment surface

after which, each one was mixed and reduced to quantities of less than 50g. The sample produced was then divided into two parts

a) the first was subjected to mineralization by adopting chemical agents assisted by a microwave source in accordance with EPA 3052 1996 for chemical elements evaluation shown in Table

Parameter	Concentration in mg/kg
	JGW
Antimony	0.2
Arsenic	15.2
Beryllium	-
Cadmium	0.11
Calcium	70350
Cobalt	10.5
Chromium total	21.1
Iron	13300
Magnesium	4750
Manganese	4.5
Nickel	11.5
Piombo	0.8
Silicon	185150
Rame (total)	19.5
Nitruro di Titanio	4.4
Vanadium	4.59
Zinc	70.5

CHEMICAL COMPOSITION of JGW and LEACHING TEST

Leaching Test

The samples of grided JTW were prepared in compliance with UNI 10802:2013.

Each sample was dried to minimize losses due to adhesion between the material and the equipment surface

after which, each one was mixed and reduced to quantities of less than 50g. The sample produced was then divided into two parts

a) the first was subjected to mineralization by adopting chemical agents assisted by a microwave source in accordance with EPA 3052 1996 for chemical elements evaluation

b) the second part was adopted for the leaching test, which was conducted at 20 ± 5°C according to EN 12457-2.

The leaching test consisted of some steps, as follows: a) the metal elements were sought in the eluate by adopting the procedure described in EN ISO 11885 (2009),

so the plasma optical emission spectrometry was used;

the dissolved solids were calculated in accordance with EN 15216;

the COD (Chemical Oxygen Demand) was defined as a portion of eluate by adopting the APAT CNR IRSA 5130 Man. 29/03 method

CHEMICAL COMPOSITION of JGW and LEACHING TEST

Leaching Test

Leaching test results, shown in Figure, demonstrate how JGW does not exceed the environmental requirements fixed by the Italian Ministerial Decree mentioned above, and they may be used for making road asphalt mixtures, partly substituting the limestone aggregates

b) c)

Figure 4 Leaching test: a) C.O.D. tritation, b) APAT CNR IRSA 5130 Man. 29/03, and c) agitation device

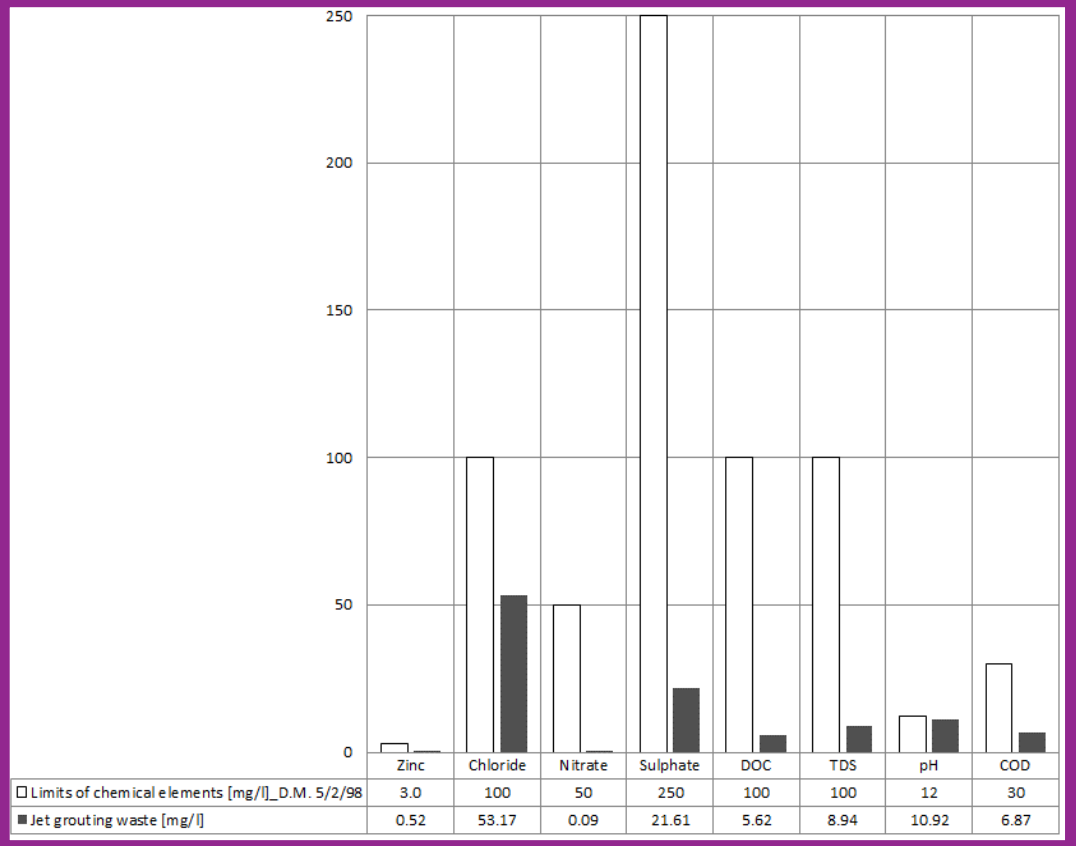

	Zinc	Chloride	Nitrate	Sulphate	DOC	TDS	pH	COD
Limits of chemical elements [mg/l]_D.M. 5/2/98	3.0	100	50	250	100	100	12	30
Jet grouting waste [mg/l]	0.52	53.17	0.09	21.61	5.62	8.94	10.92	6.87

OSSERVAZIONI AL MICROSCOPIO OTTICO

JET GROUTING WASTE

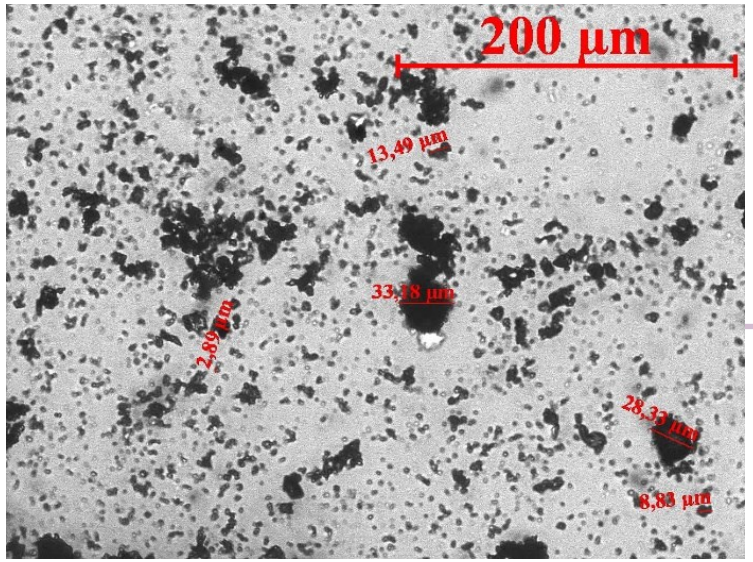

(max 126,0- min 12,7) µm

LIMESTONE SAMPLE

Particelle con contorni aguzzi (10,3-62) µm – Sferette (8-21) µm –

(…..si tratta di forme cristalline sferiche di carbonato di Calcio)

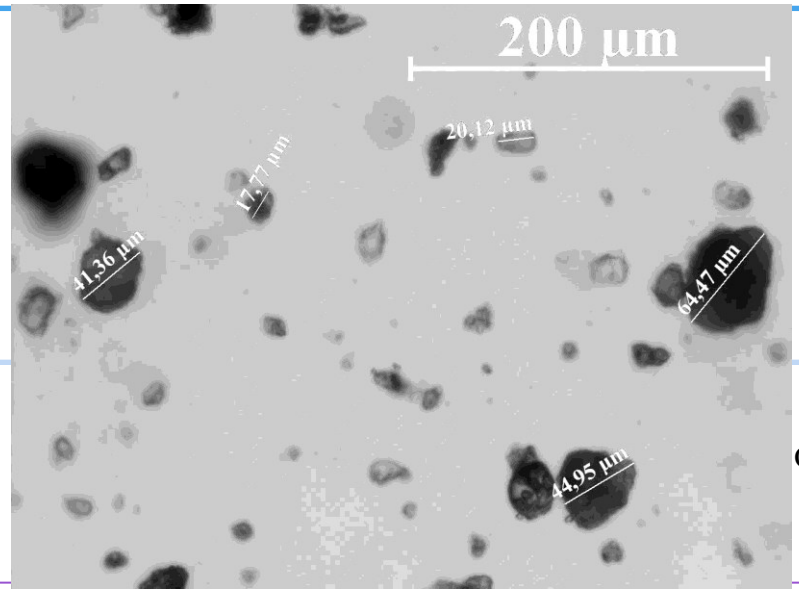

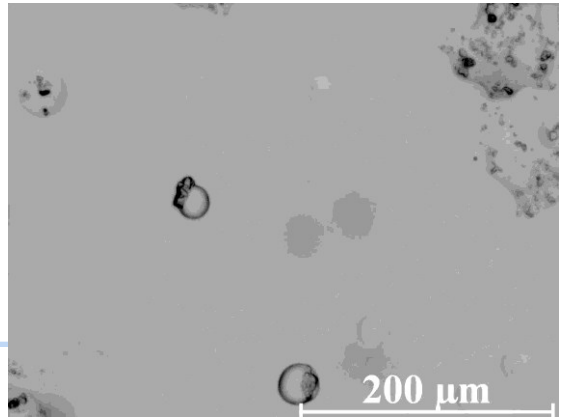

Oltre alle particelle con contorni irregolare si osservano sfere

OSSERVAZIONI della morfologia delle particelle al Microscopio SEM

Il **microscopio SEM** non sfrutta la luce **come** sorgente di radiazioni. Il fascio viene generato da una sorgente elettronica, tipicamente un filamento in Tungsteno, che emette un flusso di elettroni primari concentrato da una serie di lenti elettromagnetiche e deflesso da una lente obiettivo.

Il SEM offre una risoluzione nell'ordine di pochi nm, mentre i sistemi ottici spesso non scendono sotto i 200 nm

JET GROUTING WASTE

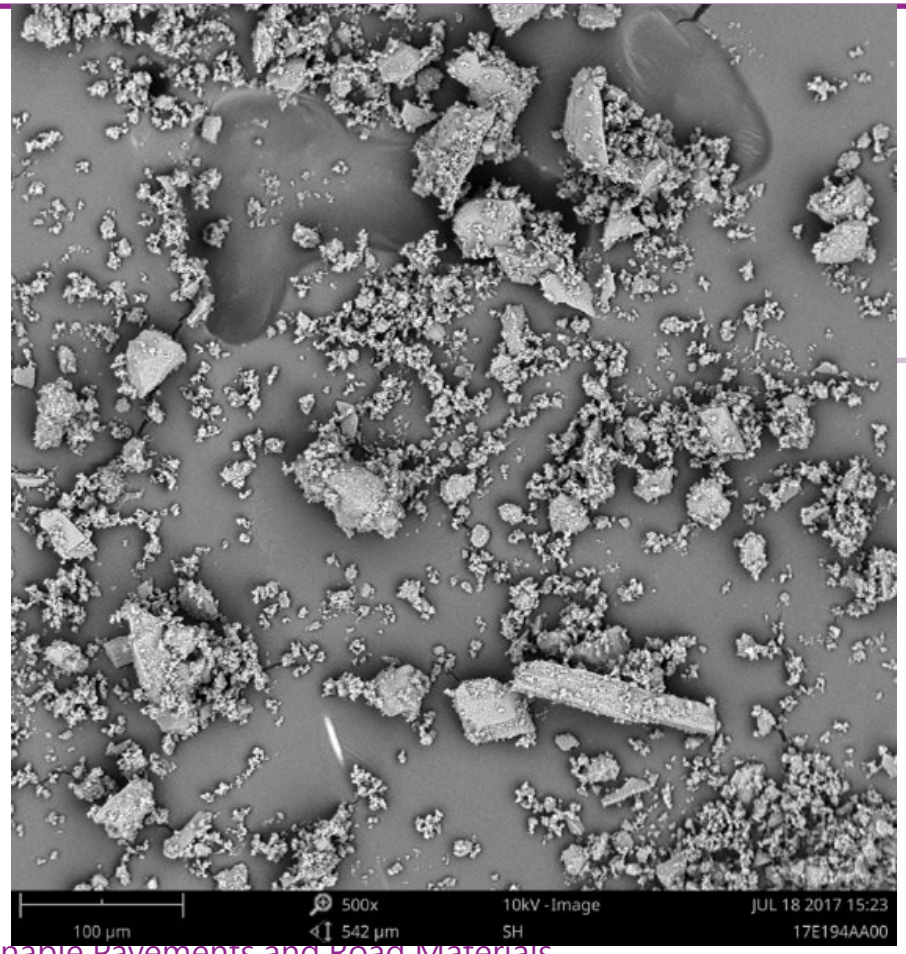

LIMESTONE SAMPLE

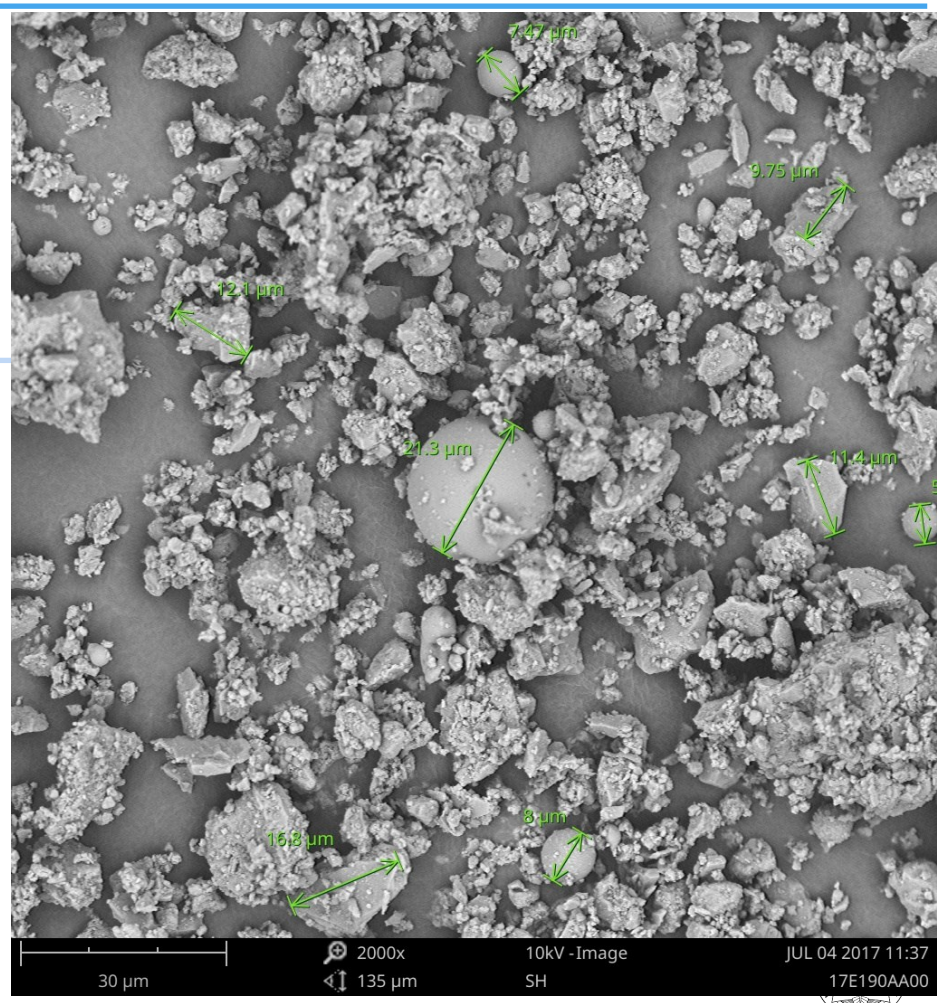

SEM+EDS (spettrometria per dispersione di energia)

L’analisi chimica (microanalisi) nel microscopio elettronico (SEM) a scansione viene realizzata misurando l’energia e la distribuzione delle intensità dei raggi X generati dal fascio elettronico sul campione utilizzando un rivelatore a dispersione di energia EDS (spettrometria per dispersione di energia).

permette di individuarne la tipologia e l’origine dei componenti

SEM+EDS (spettrometria per dispersione di energia)

L'analisi chimica (microanalisi) nel microscopio elettronico (SEM) a scansione viene realizzata misurando l'energia e la distribuzione delle intensità dei raggi X generati dal fascio elettronico sul campione utilizzando un rivelatore a dispersione di energia EDS (spettrometria per dispersione di energia).

permette di individuarne la tipologia e l'origine dei componenti

JET GROUTING WASTE

Element	Atomic % Concentration
Si	3.8
O	39.1
C	51.7
Ca	2.1
Al	1.7
K	0.5
Fe	0.4
Mg	0.2
Na	0.4

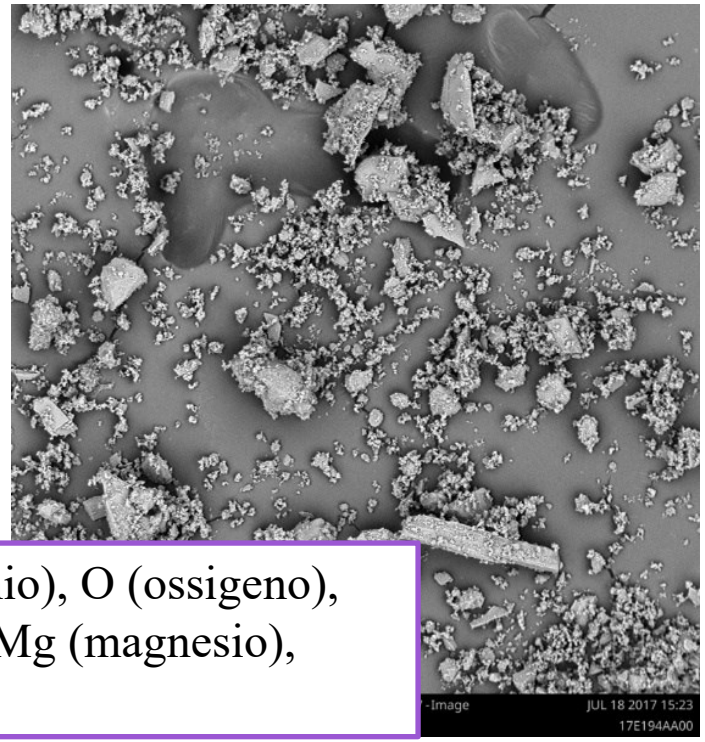

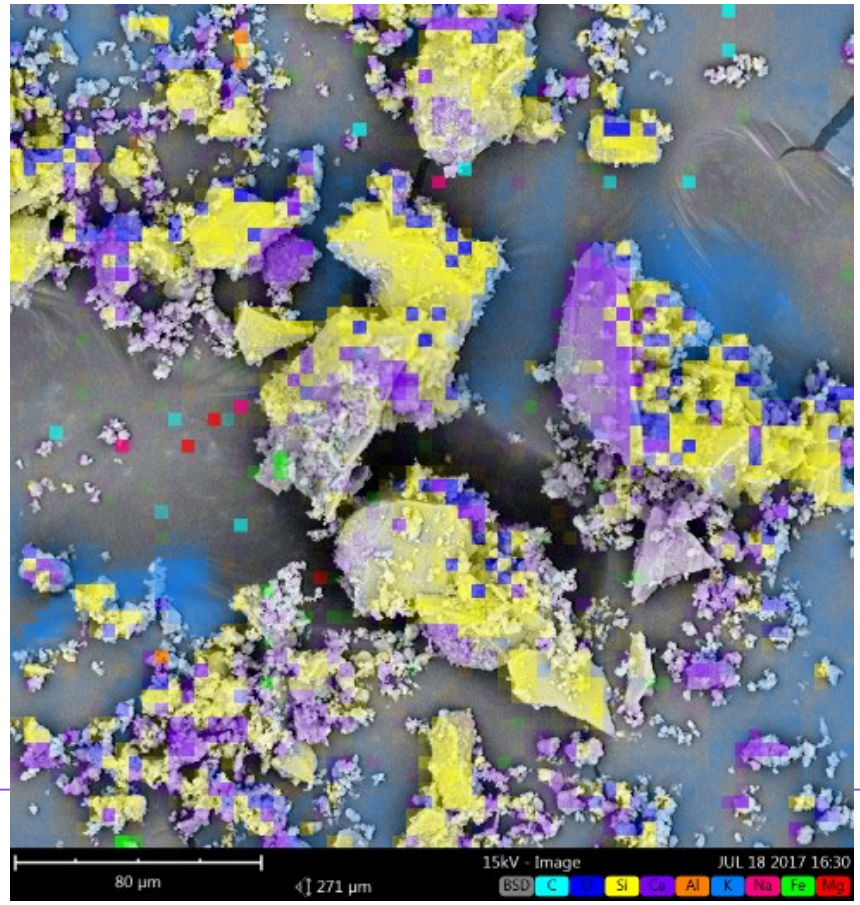

(Elementi leggeri: solitamente C (carbonio), O (ossigeno), Si (silicio), Al (alluminio), Ca (calcio), Mg (magnesio), Na (sodio), K (potassio), ….)

SEM+EDS (spettrometria per dispersione di energia)

L'analisi chimica (microanalisi) nel microscopio elettronico (SEM) a scansione viene realizzata misurando l'energia e la distribuzione delle intensità dei raggi X generati dal fascio elettronico sul campione utilizzando un rivelatore a dispersione di energia EDS (spettrometria per dispersione di energia).

permette di individuarne la tipologia e l'origine dei componenti

LIMESTONE AGGREGATES

Element	Atomic % Concentration
Ca	6.8
Si	4.5
O	48.5
Al	2.8
C	35.7
K	0.7
Fe	0.5
Mg	0.3
Na	0.3

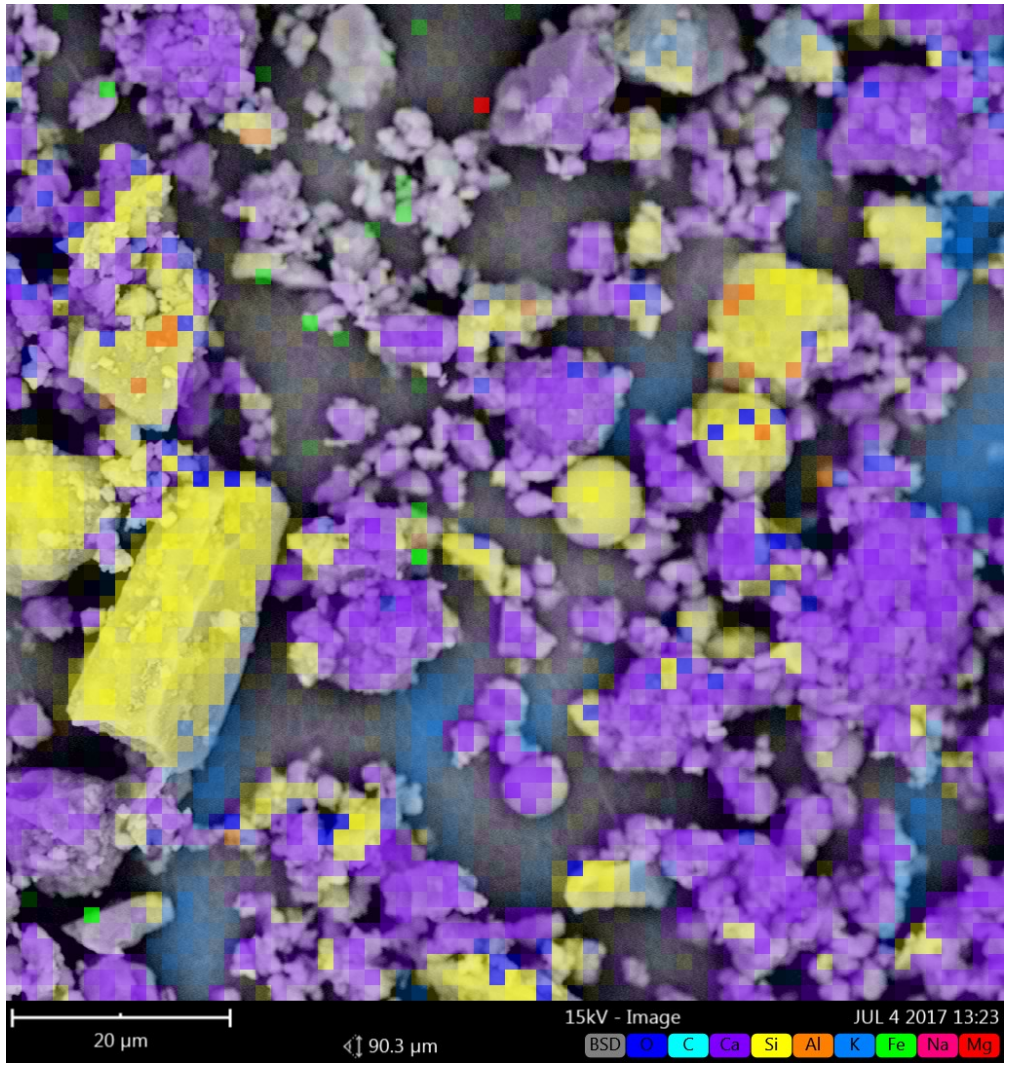

(Elementi leggeri: solitamente C (carbonio), O (ossigeno), Si (silicio), Al (alluminio), Ca (calcio), Mg (magnesio), Na (sodio), K (potassio), ….)

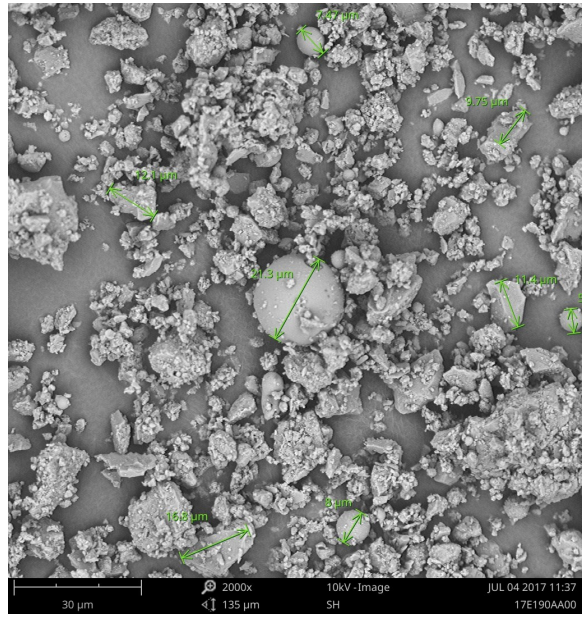

SEM+EDS (spettrometria per dispersione di energia)

L'analisi chimica (microanalisi) nel microscopio elettronico (SEM) a scansione viene realizzata misurando l'energia e la distribuzione delle intensità dei raggi X generati dal fascio elettronico sul campione utilizzando un rivelatore a dispersione di energia EDS (spettrometria per dispersione di energia).

permette di individuarne la tipologia e l'origine dei componenti

JET GROUTING WASTE

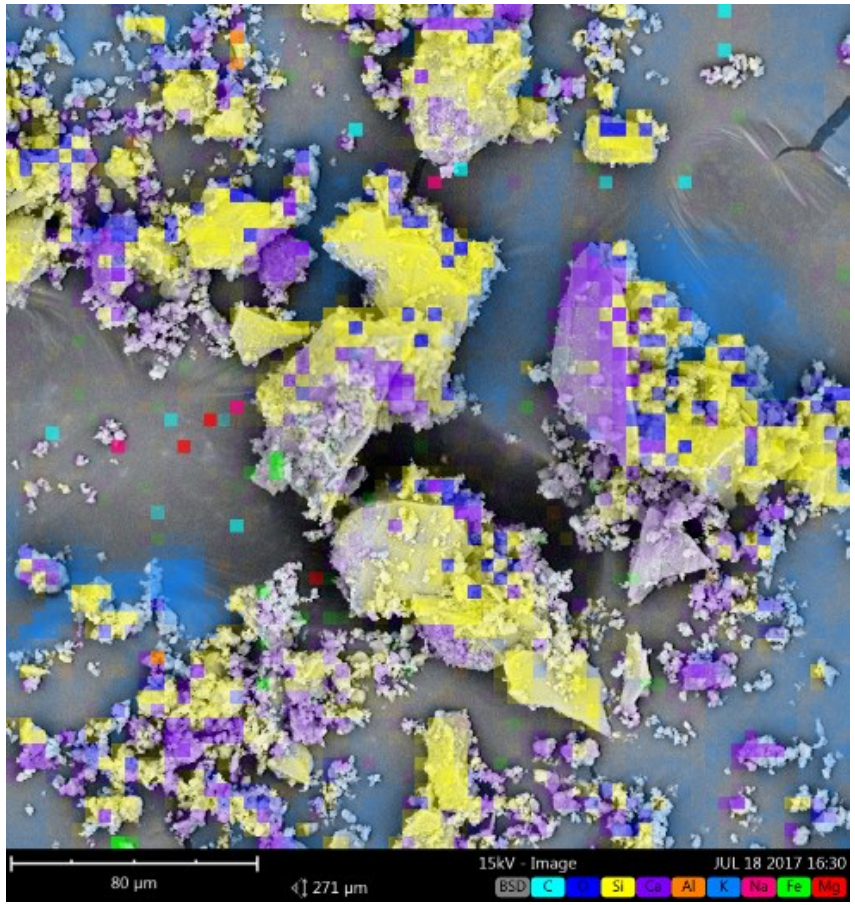

LIMESTONE AGGREGATES

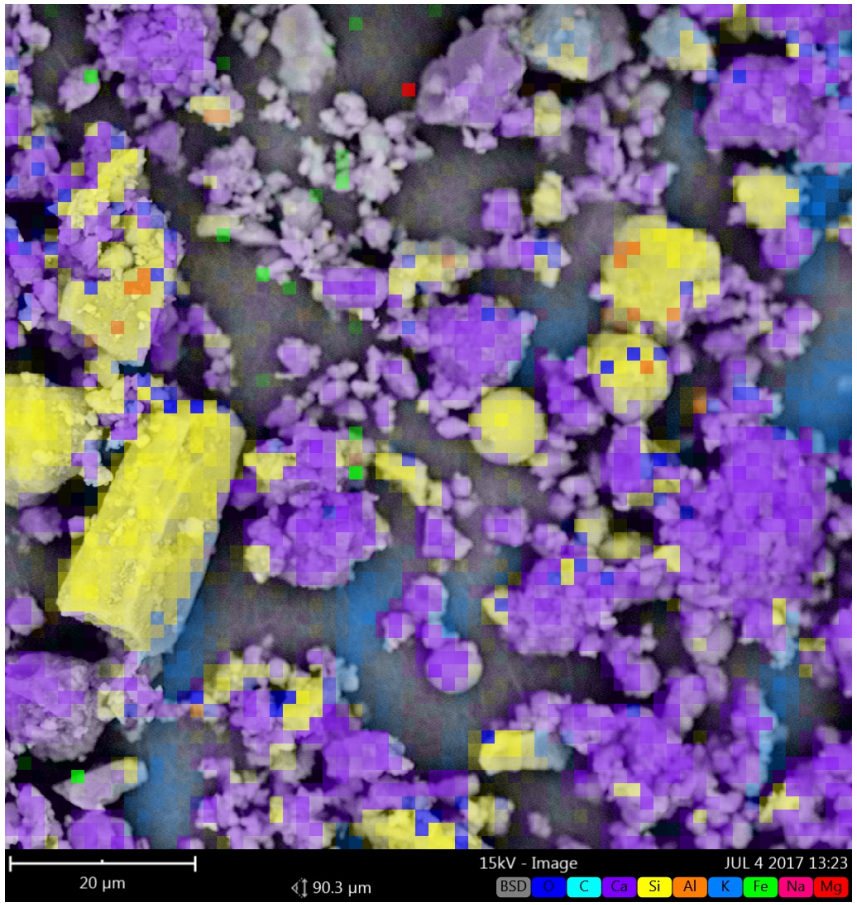

Investigating hot asphalt mastics

Binder properties

Parameters	Unit	Value	Standard
Penetration @ 25 °C	dmm	68	EN 1426
Softening point	°C	48.8	EN 1427
Dynamic viscosity @ 150°C	Pa s	0.25	EN 13702

Binder properties

Parameters	Unit	Value	Standard
Penetration @ 25 °C	dmm	68	EN 1426
Softening point	°C	48.8	EN 1427
Dynamic viscosity @ 150°C	Pa s	0.25	EN 13702

MIXING procedure

Filler-to-bitumen weight ratio (f/b) equal to 1.4

80 g bitumen | 112 g filler

↓

Three asphalt mastics were made

adding traditional limestone filler to neat B5070:LF | adding JGW as a filler to neat bitumen (B5070): JW | adding 50% Limestone filler + 50% JGW to B50/70

↓

bitumen was pre-heated in a metal container at 150 °C for 1 h and then poured into a steel container previously oven heated to 150 °C.

↓

The filler was weighed and placed in an aluminium container before being gradually poured into the bitumen. The whole blend was mixed at 4,500 rpm.

↓

Four samples were compared to define the optimal blending time of the mastics: 10, 15, 30, and 60 min mixing time.

↓

No substantial differences were noted upon increasing mixing time in terms of R&B, penetration at 25°C or dynamic viscosity at 100°C (UNI EN 13702)

↓

so, to save time and resources, a period of 10-minutes was selected for the preparation of all the mastics used in the study.

FREQUENCY SWEEP TEST (EN 14770)

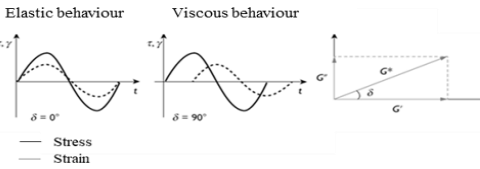

$$G^* = \frac{\tau_{max}}{\gamma_{max}}$$

- τ_{max} is the maximum value of the shear stress, kPa
- γ_{max} is the maximum value of the shear strain identified through an LVE analysis, %
- G' is the storage modulus, kPa
- G'' is the loss modulus, kPa

FREQUENCY SWEEP TEST (EN 14770)

frequency values falling within a range from 0.1 to 10 Hz

(a total of 20 observations were made with a gap of 0.1 for frequencies) passing through 1.59 Hz

at six test temperatures (10, 20, 30, 40, 50, 60°C)

A ‘‘25 mm plate-plate geometry” with a 1 mm gap was adopted to carry out the rheological analysis at test temperatures above 30°C

while ‘‘8 mm plate-plate geometry” with a 2 mm gap as the DSR configuration was used to investigate all the solutions at test temperatures below 30 °C.

In line with UNI EN 14770, it was verified that at 30 °C, which marks the crossing DSR configurations mentioned above, the values of the G* shear modulus under the two different configurations mentioned did not differ more than 15%, and the value of the phase angle did not differ by more than 3°.

In compliance with UNI EN 14770, before moving on to the FS test, a viscoelastic linear region (LVE) was identified setting out a number of three conditions as follows:

a) strain sweep was evaluated under a ‘‘25 mm plate-plate geometry” configuration at 50 °C at a frequency of 0.1 Hz;

b) strain sweep was evaluated under an ‘‘8mm plate-plate geometry” configuration at 0 °C at frequency of 10 Hz

c) making sure it fell within the LVE region, it was verified that the difference between G’ (storage modulus) and G’’ (loss modulus) did not differ more than 5% from its initial value

In order to comply with the requirements of the research study, the lowest shear strain sweep value was selected to make an effective comparison of all the bituminous samples as follows: 0.1% for a ‘‘25 mm plate-plate” configuration and 0.05% for an ‘‘8mm plate-plate” configuration.

Master curves were plotted for each mastic solution. The reference temperature was 20 °C.

Black diagrams (δ; G*) were also plotted

Mean value of the Ratios between the storage modulus G’ over the loss modulus G’’ for each mastic was assessed to identify the more or less viscous and elastic area

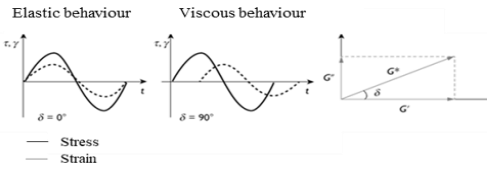

$$G^* = \frac{\tau_{max}}{\gamma_{max}}$$

- τ_{max} is the maximum value of the shear stress, kPa
- γ_{max} is the maximum value of the shear strain identified through an LVE analysis, %
- G’ is the storage modulus, kPa
- G’’ is the loss modulus, kPa

MASTER CURVES

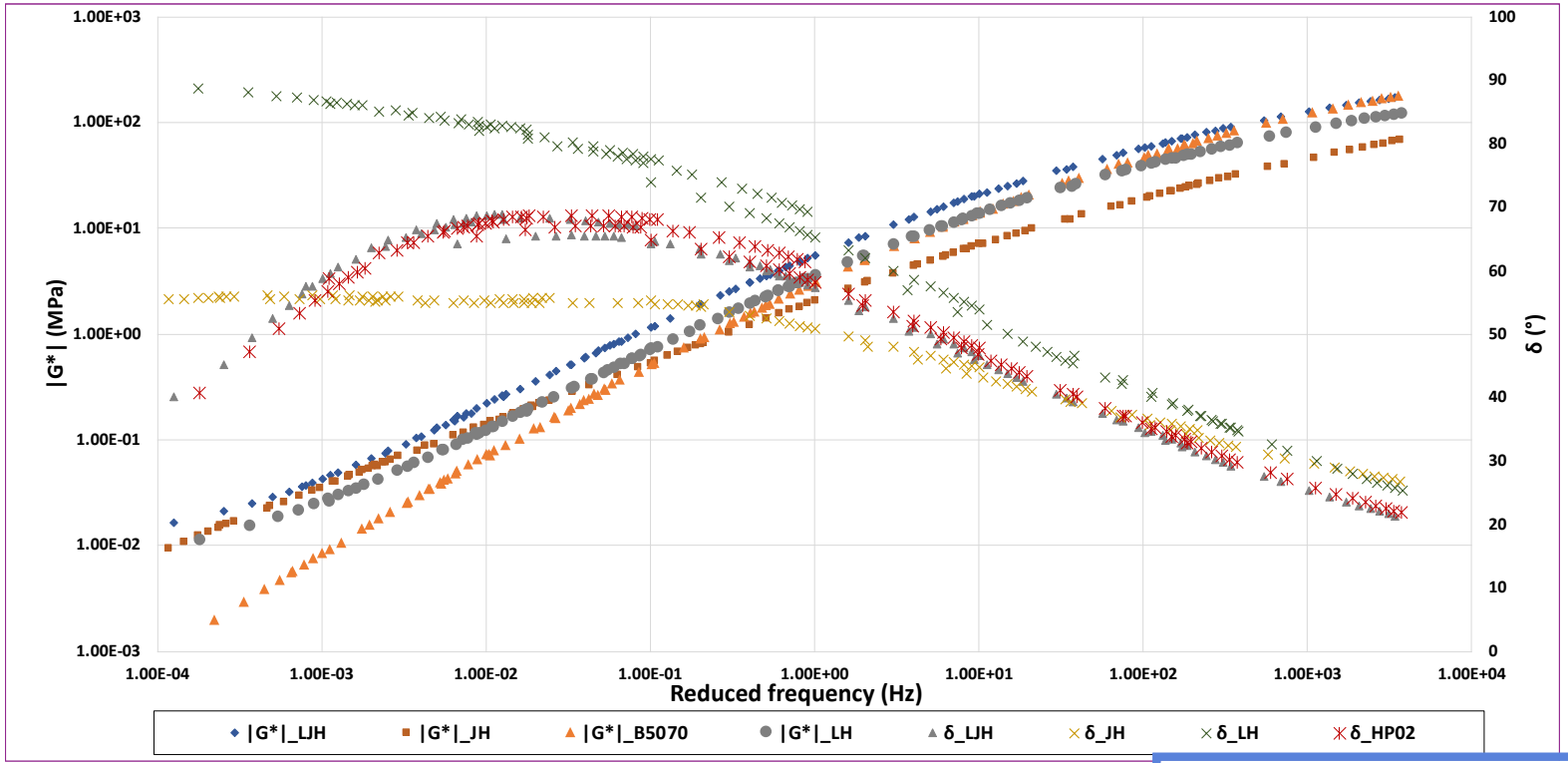

BLACK DIAGRAMS

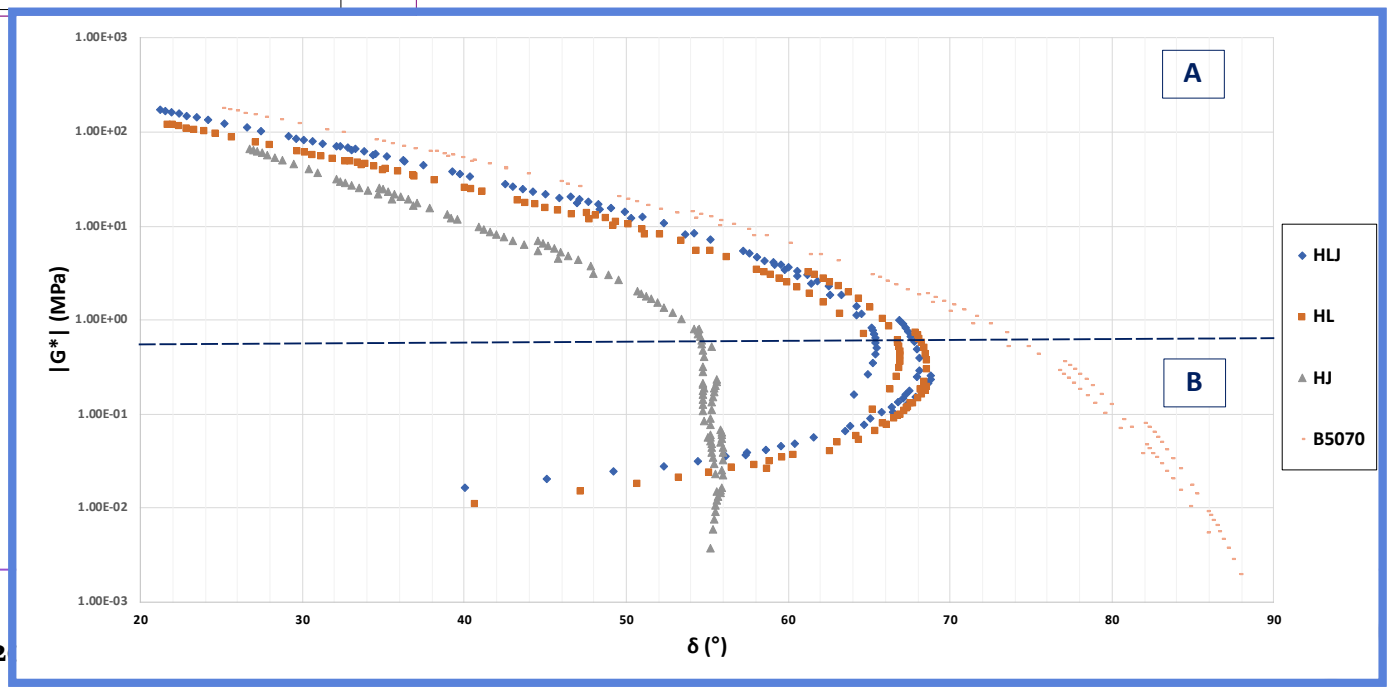

FREQUENCY SWEEP TEST (EN 14770)

T=10°C

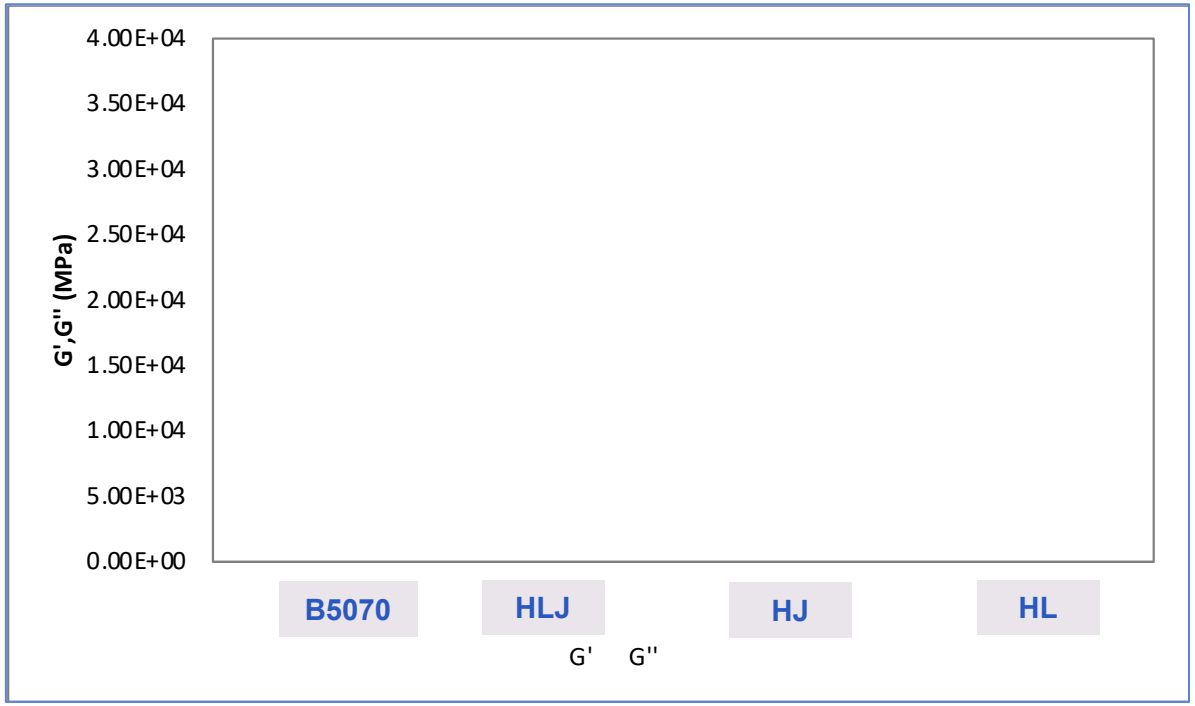

T=60°C

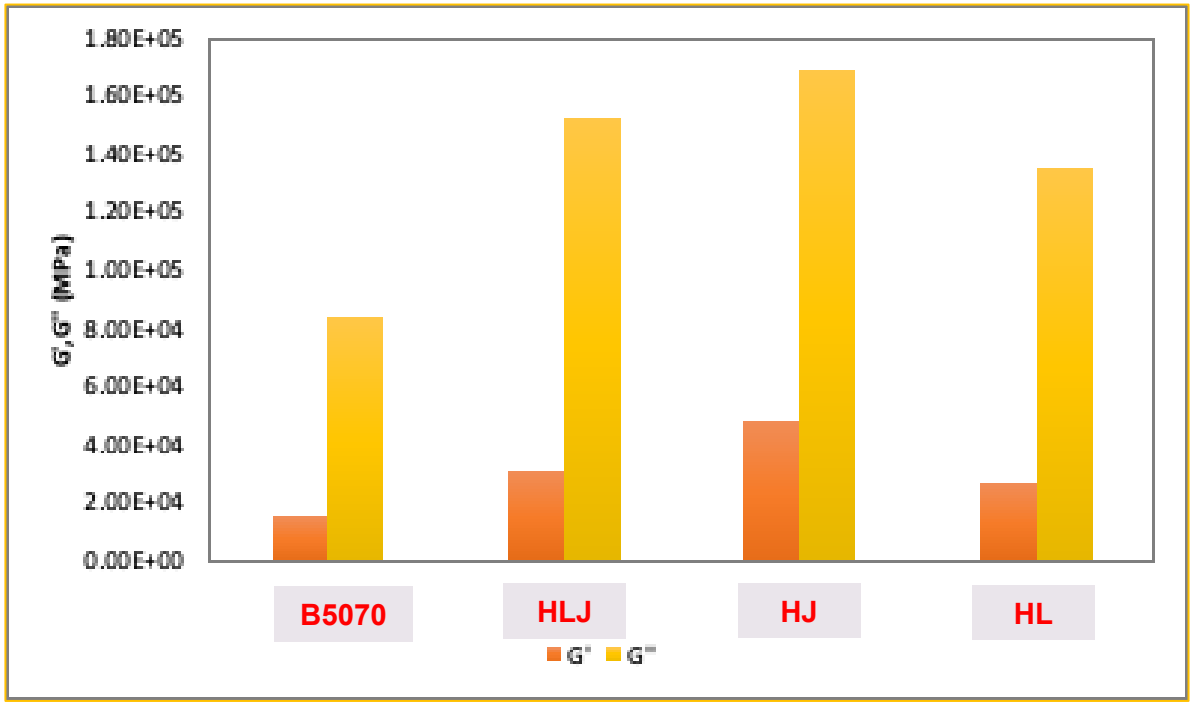

MULTI STRESS CREEP AND RECOVERY TEST (EN 16659)

Non-recoverable creep compliance (Jnr), which is one of the parameters that gives a measure of the degree of resistance of a bituminous mastic and/or binder to permanent deformations under repeated loading–unloading cycles

Two stress levels (0.1 kPa and 3.2 kPa) and two test temperatures (40 °C

and 60°C) were used

Each cycle consists in loading each specimen at constant stress for 1 sec and then unloading for 9 secs.

Ten creep and recovery cycles were carried out at 0.1 kPa, followed by a further 10 cycles at 3.2 kPa.

A 25 mm plate-plate DSR geometry with a 1 mm gap was adopted to carry out an MSCR test;

two samples were tested for each bituminous mastic and binder solution at each test temperature.

MULTI STRESS CREEP AND RECOVERY TEST (EN 16659)

Non-recoverable creep compliance (Jnr), which is one of the parameters that gives a measure of the degree of resistance of a bituminous mastic and/or binder to permanent deformations under repeated loading–unloading cycles

wo test temperatures (40 °C

n at constant stress for 1 sec and then unloading for 9 secs.

ut at 0.1 kPa, followed by a further 10 cycles at 3.2 kPa.

mm gap was adopted to carry out an MSCR test;

mastic and binder solution at each test temperature.

The average non-recoverable creep compliance was calculated at 0.1 kPa using Eqn 3, while that at 3.2 kPa was obtained using Eqn 5.

$$J_{nr0.1kPa} = \frac{1}{10}\sum_{N=1}^{10}\left(J^{N}_{nr0.1kPa}\right)(kPa^{-1}) \quad (3)$$

where

- $J^{N}_{nr0.1kPa}$ is the non-recoverable creep compliance at the N-th cycle with 0.1 kPa creep stress, as follows:

$$J^{N}_{nr0.1kPa} = \varepsilon^{N}_{10}/0.1(kPa^{-1}) \quad (4)$$

where

- ε^{N}_{10} is the strain value at the end of recovery phase (after 10 secs) of each cycle

$$J_{nr3.2kPa} = \frac{1}{10}\sum_{N=1}^{10}\left(J^{N}_{nr3.2kPa}\right)(kPa^{-1}) \quad (5)$$

where

- $J^{N}_{nr3.2kPa}$ is the non-recoverable creep compliance at the N-th cycle with 3.2 kPa creep stress, as follows:

$$J^{N}_{nr3.2kPa} = \varepsilon^{N}_{10}/3.2(kPa^{-1}) \quad (6)$$

$$J_{nr} = \frac{\gamma}{\tau}$$

Deformazione permanente media accumulata alla fine dei cicli di scarico

Sforzo di taglio applicato

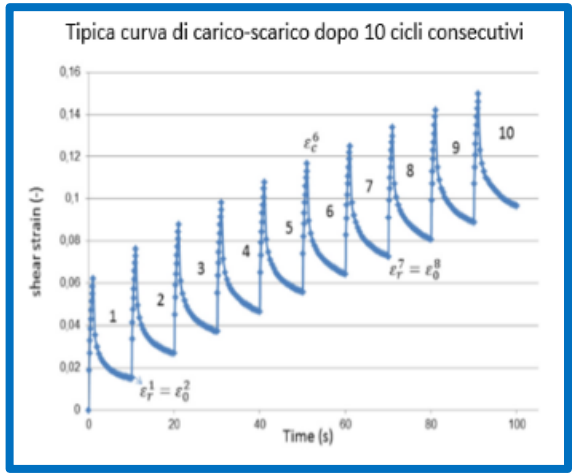

The average non-recoverable creep compliance was calculated at 0.1 kPa using Eqn 3, while that at 3.2 kPa was obtained using Eqn 5.

$$J_{nr0.1kPa} = \frac{1}{10}\sum_{N=1}^{10}\left(J^{N}_{nr0.1kPa}\right)(kPa^{-1}) \quad (3)$$

where

- $J^{N}_{nr0.1kPa}$ is the non-recoverable creep compliance at the N-th cycle with 0.1 kPa creep stress, as follows:

$$J^{N}_{nr0.1kPa} = \varepsilon^{N}_{10}/0.1(kPa^{-1}) \quad (4)$$

where

- ε^{N}_{10} is the strain value at the end of recovery phase (after 10 secs) of each cycle

$$J_{nr3.2kPa} = \frac{1}{10}\sum_{N=1}^{10}\left(J^{N}_{nr3.2kPa}\right)(kPa^{-1}) \quad (5)$$

where

- $J^{N}_{nr3.2kPa}$ is the non-recoverable creep compliance at the N-th cycle with 3.2 kPa creep stress, as follows:

$$J^{N}_{nr3.2kPa} = \varepsilon^{N}_{10}/3.2(kPa^{-1}) \quad (6)$$

The average total creep compliance was calculated at 0.1 kPa using Eqn 7, while that at 3.2 kPa was obtained from Eqn 9.

$$J_{tot0.1kPa} = \frac{1}{10}\sum_{N=1}^{10}\left(J^{N}_{tot0.1kPa}\right)(kPa^{-1}) \quad (7)$$

where

- $J^{N}_{tot0.1kPa}$ is the total creep compliance at the N-th cycle with 0.1 kPa creep stress, as follows:

$$J^{N}_{tot0.1kPa} = \varepsilon^{N}_{1}/0.1(kPa^{-1}) \quad (8)$$

where

- ε^{N}_{1} is the strain value at the end of the creep phase (after 1 sec) of each cycle

$$J_{tot3.2kPa} = \frac{1}{10}\sum_{N=1}^{10}\left(J^{N}_{tot3.2kPa}\right)(kPa^{-1}) \quad (9)$$

where

- $J^{N}_{tot3.2kPa}$ is the total creep compliance at the N-th cycle with 3.2 kPa creep stress, as follows:

$$J^{N}_{tot3.2kPa} = \varepsilon^{N}_{1}/3.2(kPa^{-1}) \quad (10)$$

MULTI STRESS CREEP AND RECOVERY TEST (EN 16659)

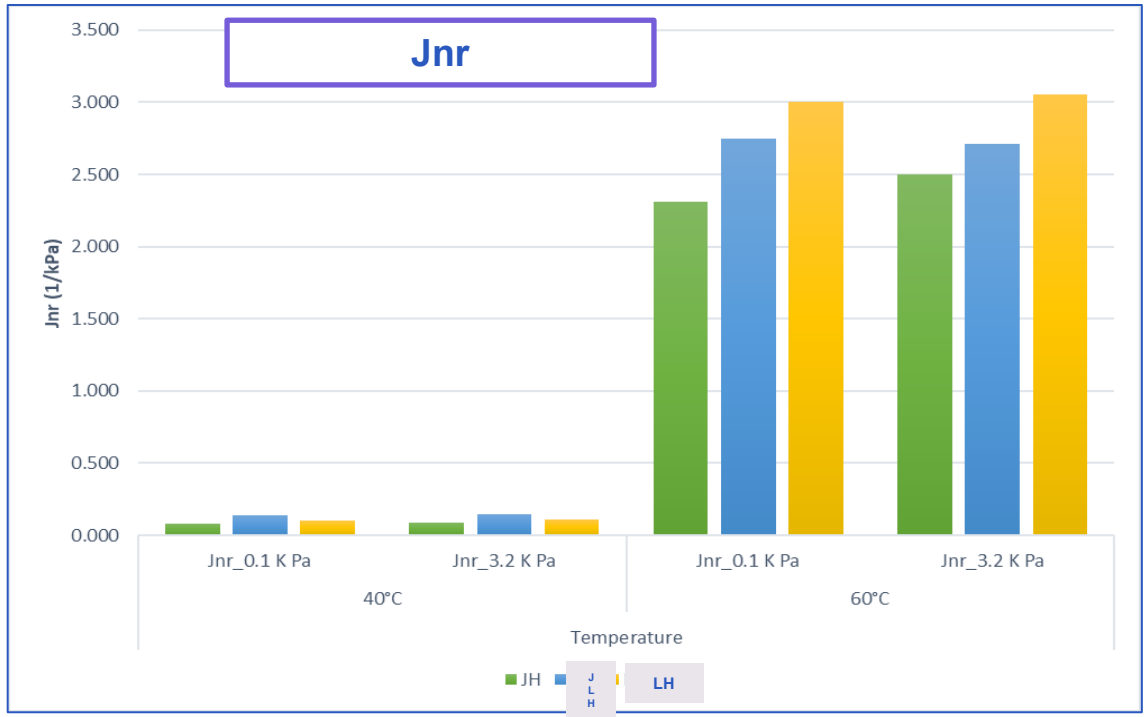

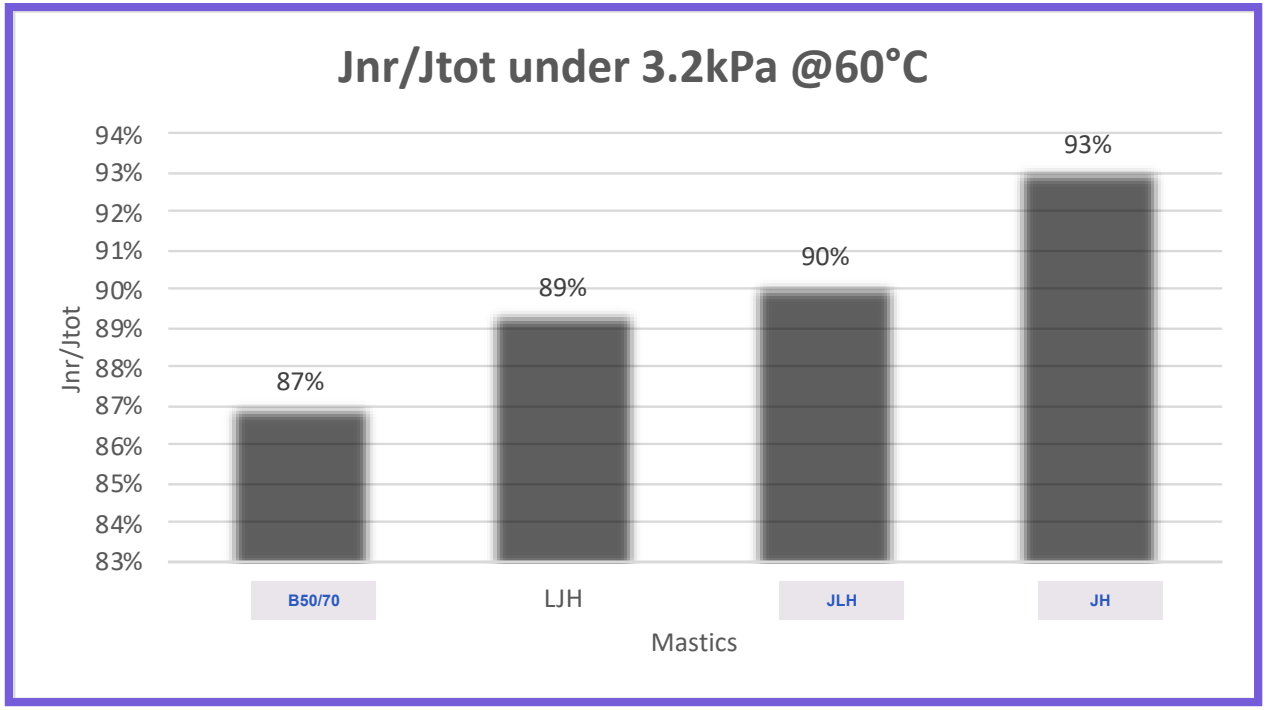

Overall, it is noted that recoverable creep compliance improves starting from B5070 in the following order: mastics made up using LF filler (averaging 30% more than B5070), mastics made up with JGW+LF as filler (averaging 84% more than B5070), mastics made up only by JGW as a filler (averaging 90% more than B5070)

The lowest permanent deformation was obtained by the hot mastic made up of JW that achieved values on average 42% lower than the hot mastic with LF that returned the highest permanent deformation value

On the whole, Jnr and Jtot appear to be thermo-dependent but not stress-dependent in all the solutions investigated

Investigating hot asphalt mixtures

GRADING CURVES

Traditional HMA

- Limestone aggregate (100%)
[of which filler – 5.6%]
- Neat Bitumen 50/70 (4 %)

by the total weight of the aggregates

HMAJ+ part Limestone filler

- Limestone aggregates (93,70%)
- Jet grouting waste (4,30%)
- Limestone filler (2%)
- Neat Bitumen 50/70 (4.5%)

HMAJ

- Limestone aggregates (93%)
- Jet grouting waste (7 %)
- Neat Bitumen 50/70 (5 %)

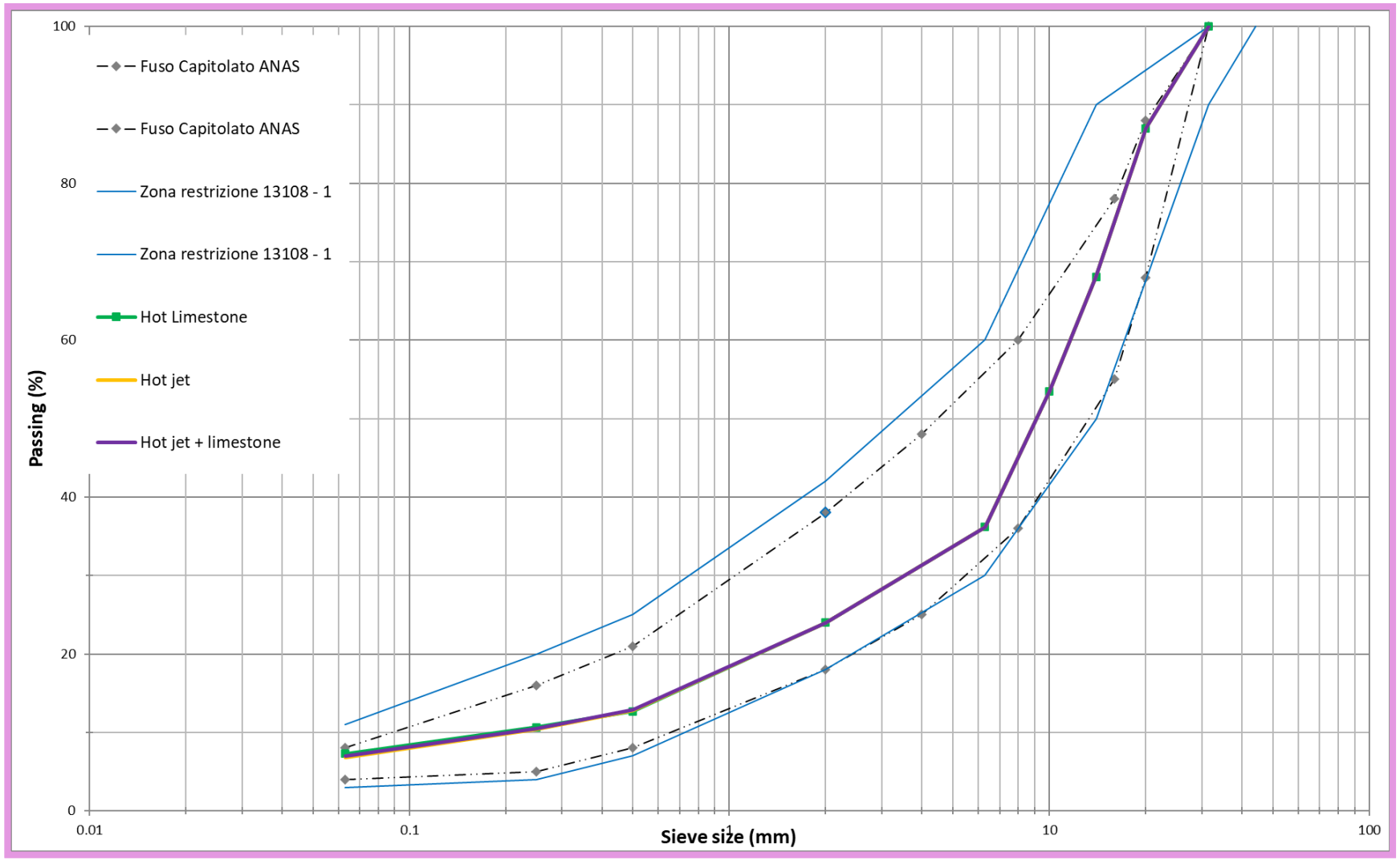

Bulk density	g/cm³	2.52

Angolo di rotazione: 1.25° ± 0.02°
Velocità di rotazione: 30 giri/min.
Pressione verticale: 600 kPa
Dimensioni provino: 150 mm
N° giri: 180

Focusing on OBC determination of HMA, HMA, HJLH solutions

a total of **18 cylindrical** specimens were prepared at 160°C under gyratory compaction energy (EN 12697-31) for each mixture

- 3 ITS 6 ITSR 5 ITSM 4 CREEP@40°C

by investigating five percentages of bitumen from 3.5 to 5.0% by the total weight of the aggregates with 0.25% increment

Cylindrical specimens with a diameter of 150mm were compacted at N_{max} number of revolutions equal to 180 and it was verified whether the percentage of air voids (EN 12697-8) was equal to 4%.

The percentage increase by 0.5% of OBC moving from HMA to HMAJ matching Rigden voids values: the Rigden voids of JGW are higher than traditional limestone filler and it leads to a percentage of intergranular voids filled by bitumen higher for HMAJ solution than HMA solution.

Resistenza a trazione Indiretta

EN 12697-23 – Temp. di prova 25°C

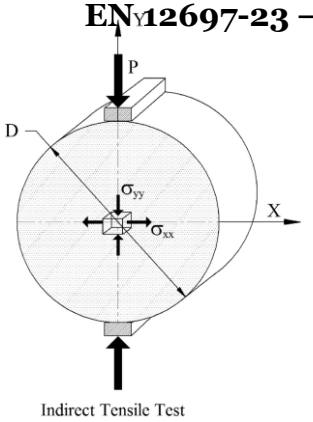

Indirect Tensile Test

$$ITS = \frac{2P}{\Pi DH}$$

where

- P is the peak load (N)
- d is the diameter of the specimen (mm)
- h is the height of the specimen (mm)

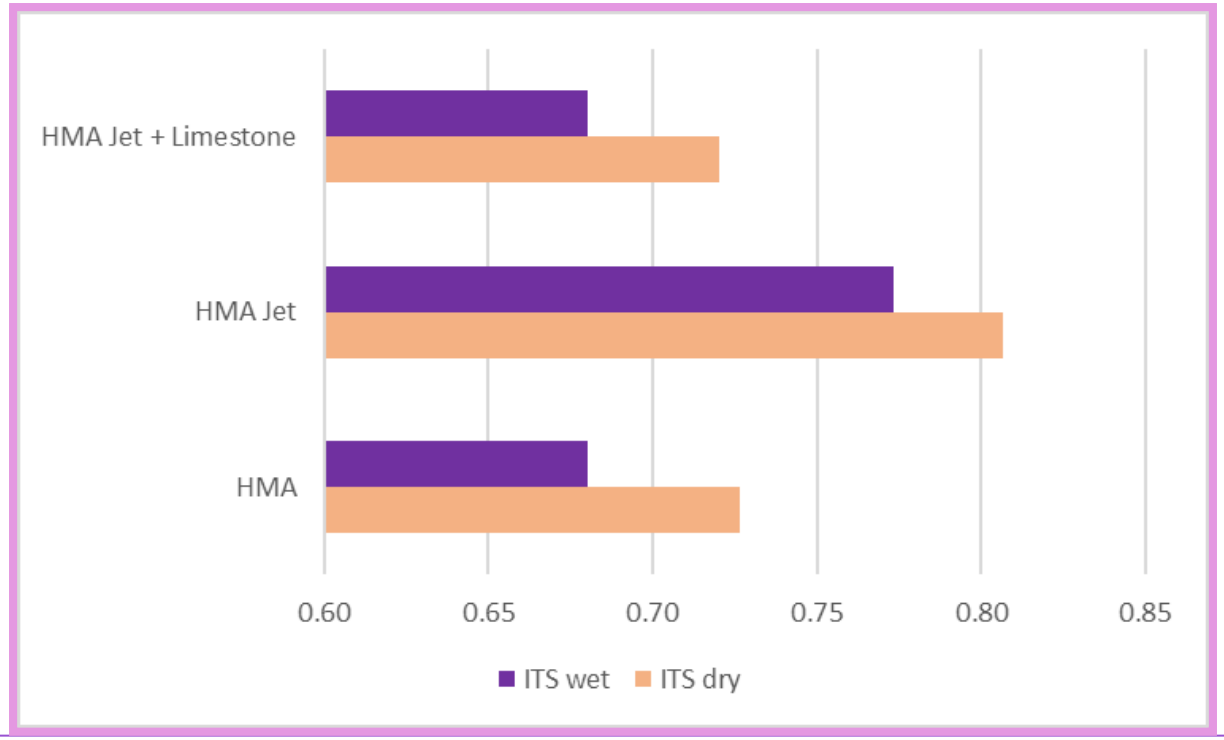

Resistenza all'acqua

EN 12697-12 – Temp. di prova 25°C

$$\mathrm{ITSR} = \frac{\mathrm{ITS_{wet}}}{\mathrm{ITS_{dry}}} \cdot 100$$

INDIRECT TENSILE STIFFNESS MODULUS (ITSM) TEST

EN 12697-26 – Annesso C

spostamento orizzontale imposto 5±0.2 µm

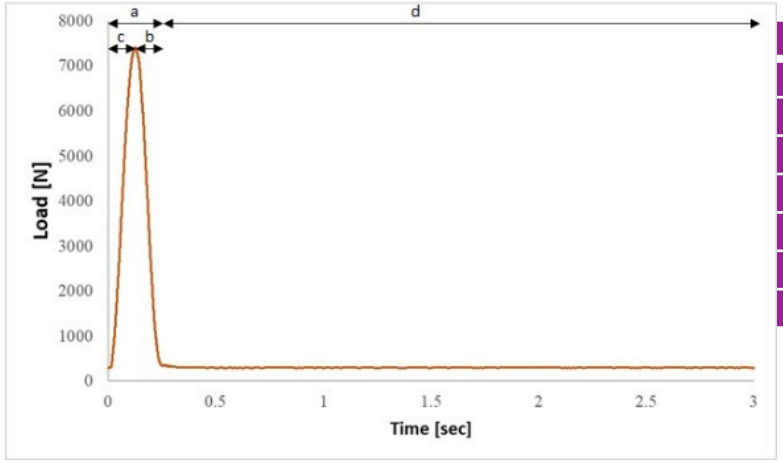

Test Parameters	Unit	Value
Loading pulse rise-time (see “c” in Figure)	ms	120
Rest period (see “d” in Figure)	ms	3000
Pulse repetition period	ms	3000
N° conditioning pulses	-	10
Target temperature	°C	10
Estimated Poisson's ratio	-	0.35
Target horizontal	µs	47

- applying an indirect tension to cylindrical specimens whose loading parameters and test configuration are shown in Table and Figure .
- Test temperatures were 10°C, 25°C, and 30°C.
- The applied load had a haversine waveform (see Figure) with a pulse load time applied for 240 milliseconds (see ‘part a of the graph’ in Figure), corresponding to a rise time of 120 milliseconds.
- Loading time consisted of two equal parts: rise time (see ‘part c’ of the graph in Figure) and unloading time (see ‘part d’ of the graph in Figure).
- Each load pulse was followed by an unloaded period (see ‘part b’ of the graph in Figure).
- A total of 5 pulses were applied for stiffness measurements

INDIRECT TENSILE STIFFNESS MODULUS (ITSM) TEST

EN 12697-26 – Annesso C

spostamento orizzontale imposto 5±0.2 µm

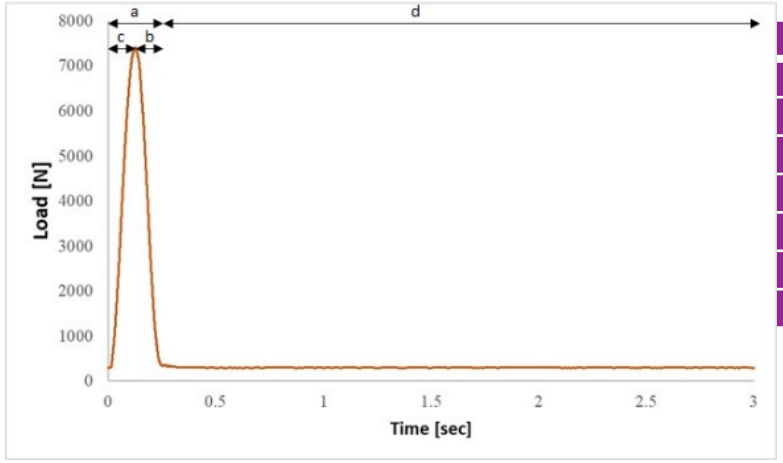

Test Parameters	Unit	Value
Loading pulse rise-time (see "c" in Figure)	ms	120
Rest period (see "d" in Figure)	ms	3000
Pulse repetition period	ms	3000
N° conditioning pulses	-	10
Target temperature	°C	10
Estimated Poisson's ratio	-	0.35
Target horizontal	µs	47

- applying an indirect tension to cylindrical specimens whose loading parameters and test configuration are shown in Table and Figure .
- Test temperatures were 10°C, 25°C, and 30°C.
- The applied load had a haversine waveform (see Figure) with a pulse load time applied for 240 milliseconds (see 'part a of the graph' in Figure), corresponding to a rise time of 120 milliseconds.
- Loading time consisted of two equal parts: rise time (see 'part c' of the graph in Figure) and unloading time (see 'part d' of the graph in Figure).
- Each load pulse was followed by an unloaded period (see 'part b' of the graph in Figure).
- A total of 5 pulses were applied for stiffness measurements

Using the measurements from the 5 load pulses, ITSM, in MPa, shall be determined using following Equation 2.

$$ITSM = \frac{F \cdot (v+0.27)}{(z \cdot h)} \rightarrow (\text{MPa}) \quad -$$

Where
F is the peak value of the applied vertical load,in N;
z is the amplitude of the horizontal deformation obtained during the load cycle, in mm;
h is the thickness of the specimen, equal to 60 mm;
v is the Poisson's ratio, equal to 0.35.
As prescribed by EN 12697-26, all measurements were performed at a strain level of less than 50 micro-strains in order to be in the linear viscoelastic zone.

INDIRECT TENSILE STIFFNESS MODULUS (ITSM) TEST

EN 12697-26 – Annesso C

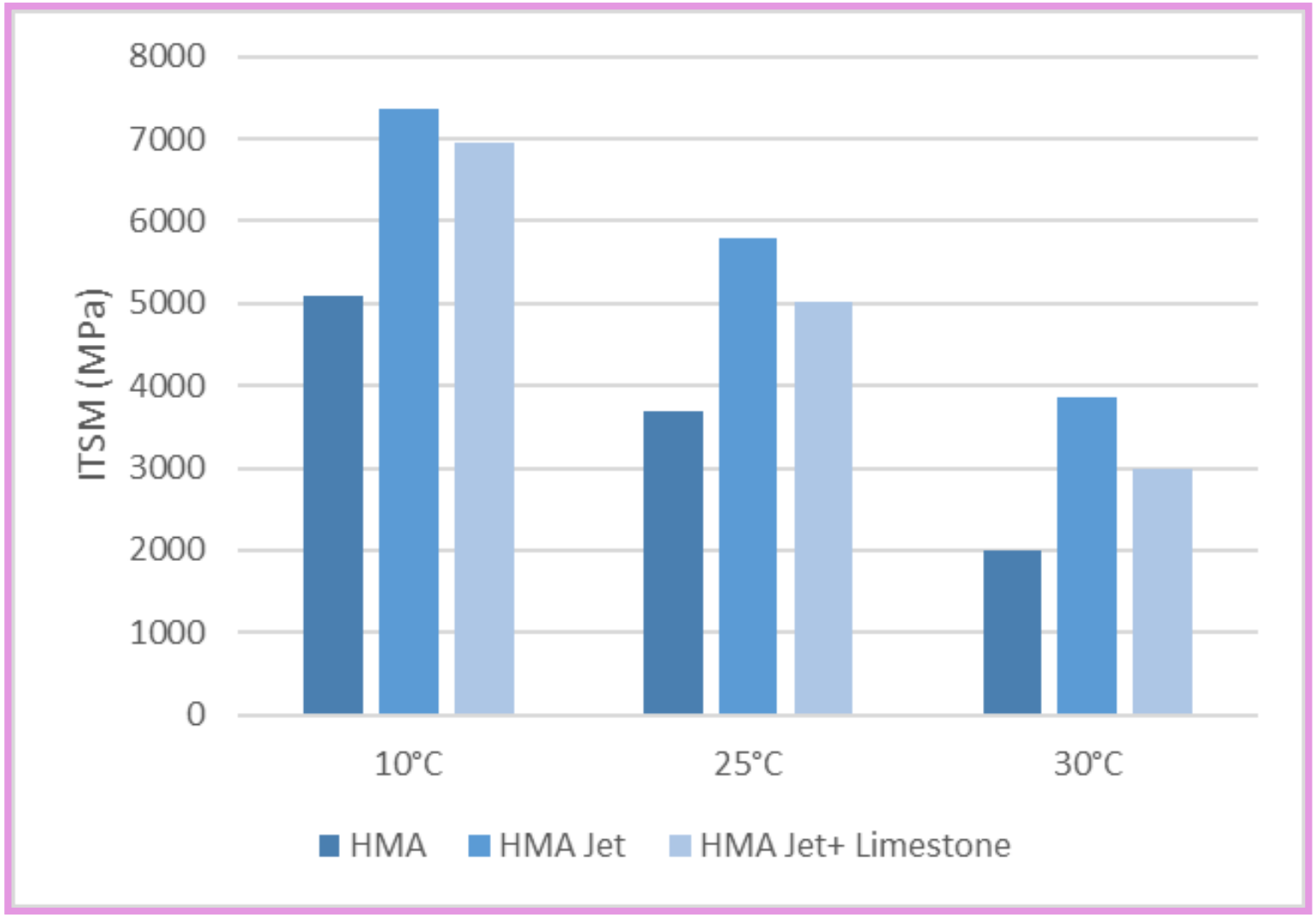

VERIFICA DI RESISTENZA ALL'ACCUMULO DI DEFORMAZIONI PERMANENTI

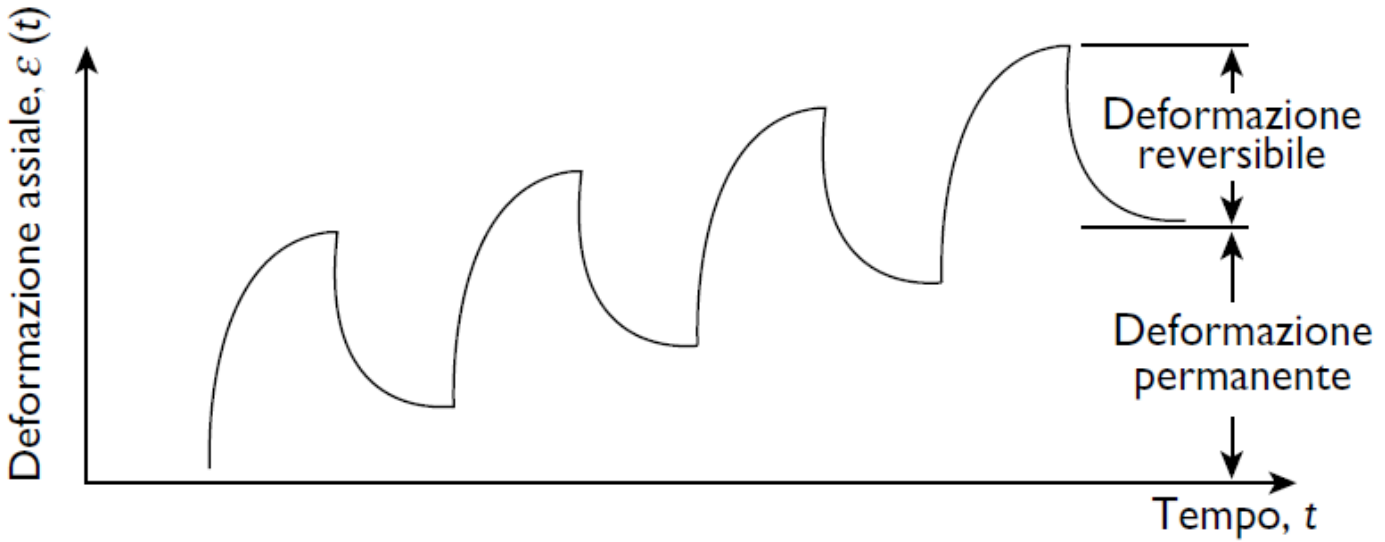

GLI EFFETTI CONSEGUENTI AL RIPETUTO PASSAGGIO DI VEICOLI

SI TRADUCONO PER OGNI CICLO IN DEFORMAZIONE,

CHE NELLA FASE DI RIPOSO VIENE RECUPERATA PARZIALMENTE DANDO LUOGO A UN PROGRESSIVO ACCUMULO DI DEFORMAZIONI PERMANENTI

PROVA DI COMPRESSIONE CICLICA TRIASSIALE CON CONFINAMENTO PER DETERMINARE LE CARATTERISTICHE DI CREEP DI MISCELE BITUMINOSE (EN 12697-25)

- campione cilindrico sottoposto a un carico assiale ciclico ripetuto
- pressione di contenimento laterale applicata
- Durante la prova è misurata la variazione dell'altezza del campione $\varepsilon_n = 100 \cdot (h_0 - h_n)/h_0$
  - la deformazione assiale cumulata (permanente) del provino è determinata in funzione del numero di applicazioni di carico
- I campioni possono essere preparati in laboratorio o essere estratti dalla parte centrale di una pavimentazione

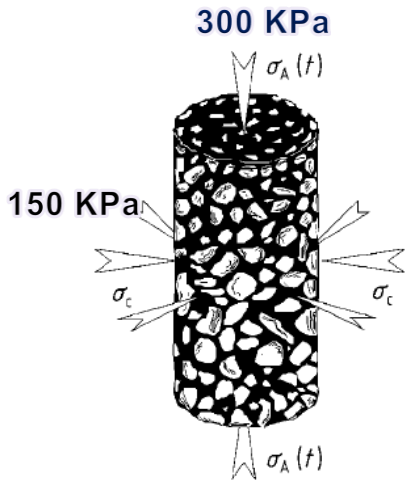

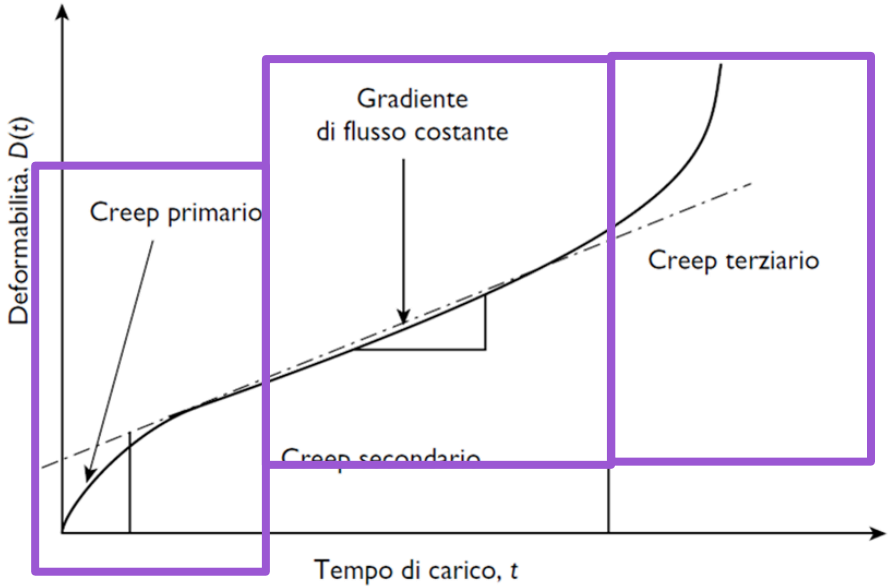

L'estensione delle regioni di deformabilità dipende da diversi fattori, quali
l'entità del carico applicato,
temperatura
frequenza
proprietà degli inerti
quantità e tipologia di filler
caratteristiche reologiche del legante e dei mastici

TRIAXIAL CYCLIC COMPRESSION TEST @40°C

(UNI EN 12697-25)

$$\sigma_C + \sigma_a(t) = \sigma_C + \sigma_V \cdot (1 + sin(2\pi \cdot f \cdot t))$$

where

- σ_C is the confining stress (all around the specimen), kPa
- $\sigma_a(t)$ is the cyclic axial pressure as a function of time, kPa
- σ_V is the amplitude of the haversinusoidal pressure, kPa
- f is the frequency, Hz
- t is the time

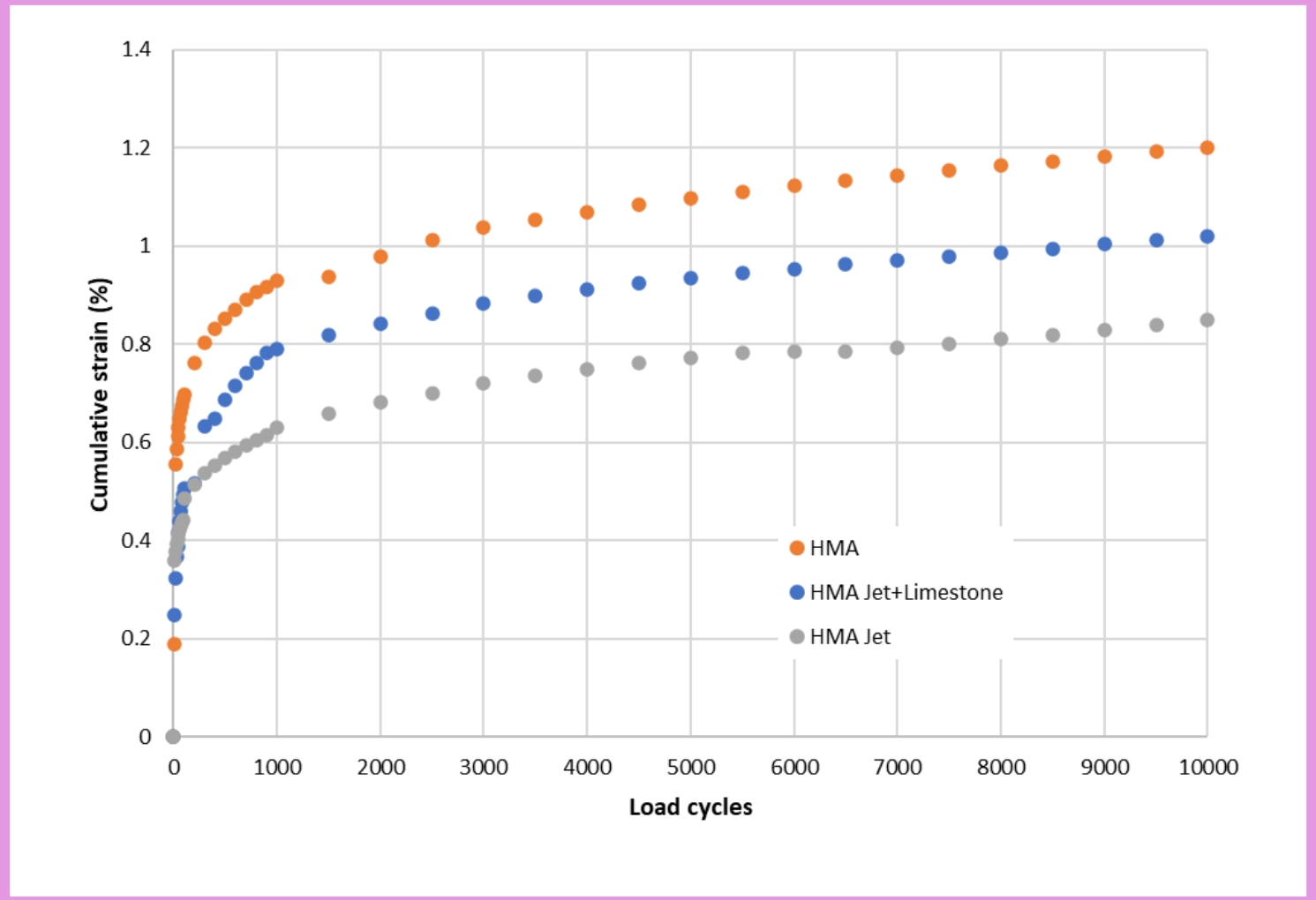

VERIFICA DI RESISTENZA ALL'ACCUMULO DI DEFORMAZIONI PERMANENTI

CALCOLO ORMAIA PER SINGOLA LASTRA DI MISCELA IN CONGLOMERATO BITUMINOSO SECONDO IL METODO DELLA TRACCIA DELLE RUOTE (WHEEL TRACKING, EN 12697-22

LASTRA (40X30cm - 19,5cm H) IN C.B. COMPATTATA CON L'AUSILIO DI **ADVANCED ASPHALT SLAB ROLLER COMPACTOR** (EN 12697-33)

ADVANCED ASPHALT SLAB ROLLER COMPACTOR possono compattare lastre di C.B. ad una densità target, applicando carichi specifici corrispondenti a quelli dei rulli nella costruzione di pavimentazioni stradali.

La lastra può essere utilizzata per

- Wheel tracking test
- Cored to provide specimens for indirect tensile, static and dynamic creep tests
- Cut into beams for fatigue tests

- I compattatori di lastre elettromeccanici sono dotati di un sistema di compattazione a rulli con raggio di testa del segmento 535 mm;
- il carico verticale è applicato ortogonalmente all'asse del moto di traslazione. Max vertical force 30kN
- il carrello portastampi si muove avanti e indietro con un movimento lineare - Adjustable up to 300 mm/s speed - Adjustable pause at inversion point- adjustable frequency from 10 to 50 Hz

WHEEL TRACKING TEST

Double wheel tracking

Il test viene utilizzato per determinare la suscettibilità di miscele in C.B. a deformarsi sotto carico, misurando la profondità del solco formata da passaggi ripetuti di una ruota caricata a una temperatura fissa

EN prescrive l'esecuzione della prova in aria e in acqua.

Deve essere mantenuto un livello dell'acqua di circa 20 mm sopra il campione. Quando è specificato un ambiente ad aria riscaldata, il campione, durante la prova, deve essere mantenuto a una temperatura specificata uniforme e costante ± 1°C.

doppio pneumatico in gomma piena, diametro 203 mm. x 50 mm di larghezza (w). Spessore 20mm

La ruota viene spostata avanti e indietro di 230 mm sulla sommità della lastra, che è fissa.

La velocità è di 26,5 cicli al minuto (da 40 passaggi).

Ciascuna ruota è dotata di trasduttori per la misura di deformazioni da 0 a 40 mm ±0,01 mm.

La dimensione della lastra più lunga è orientata nella direzione di marcia della ruota.

Il carico della ruota deve essere di $\left[700\frac{w}{50} \pm 10\right]$N

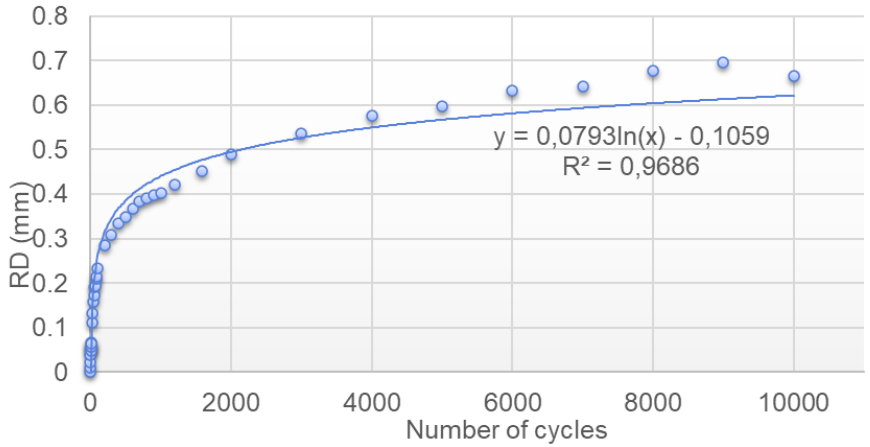

❑ Ruth depht after 1000 cycles

$$Rut\ depht\ (RD)_i = \sum_{J=1}^{20} \frac{(dij - d_{0j})}{20}$$

❑ Proportional ruth depht

$$PRD_{AIR} = 100 \frac{d_n - d_0}{h} \%$$

d_n is the vertical displacement after n load cycles, in millimetre (mm);

d_0 is the vertical displacement initially, in millimetre (mm);

h is the specimen thickness, in millimetre (mm).

	RD @60°C wet		PRD @60°C	
	Values	Distance from HMA	Values	Distance from HMA
Mixture type	[mm]	[%]	[%]	[%]
HMA	19.22		32.04	
HMA Jet	10.21	-47%	17.01	-47%
HMA Jet + Limestone	14.67	-24%	24.45	-24%

❑ Wheel-tracking slope

The wheel-tracking slope in water, in mm per 1 000 load cycles, is calculated as:

$$WTS_W = \frac{d_{10\,000} - d_{5\,000}}{5}$$

where

WTS_W is the wheel-tracking slope, in millimetres per 1 000 load cycles;

$d_{5\,000}$, $d_{10\,000}$ is the vertical displacementafter 5 000 load cycles and 10 000 load cycles, in millimetres (mm).

	RD @60°C wet		WTS @60°C	
	Values	Distance from HMA	Values	Distance from HMA
Mixture type	[mm]	[%]	mm/10^3 cicli	[%]
HMA	19.22		0.29	
HMA Jet	10.21	-47%	0.49	70%
HMA Jet + Limestone	14.67	-24%	0.84	189%

Dipartimento di Ingegneria Civile Edile e Ambientale

Università degli Studi di Napoli Federico II

Laboratorio di Strade Luigi Tocchetti

Prof.Ing.Francesca Russo

Dipartimento di Ingegneria Civile, Edile e Ambientale

RESPONSABILE del LABORATORIO DI STRADE LUIGI TOCCHETTI

Università degli Studi di Napoli Federico II - Via Claudio 21-

francesca.russo2@unina.it

https://www.facebook.com/laboratorioLaSTra/

Grazie della vostra cortese attenzione

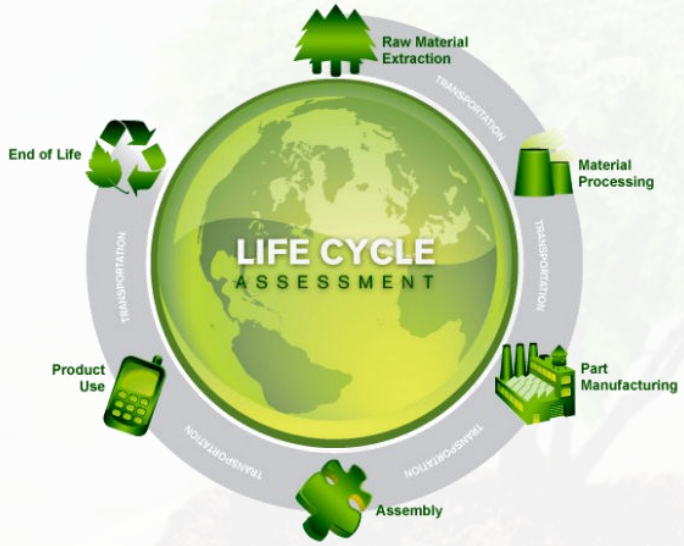

Life Cycle Assessment

Life Cycle Assessment

The Life Cycle Assessment (**LCA**) is a method that evaluates the set of interactions that a product or service has with the environment, considering its entire life cycle which includes the pre-production phases (therefore also the extraction and production of materials), production, distribution, use (therefore also reuse and maintenance), recycling and final disposal

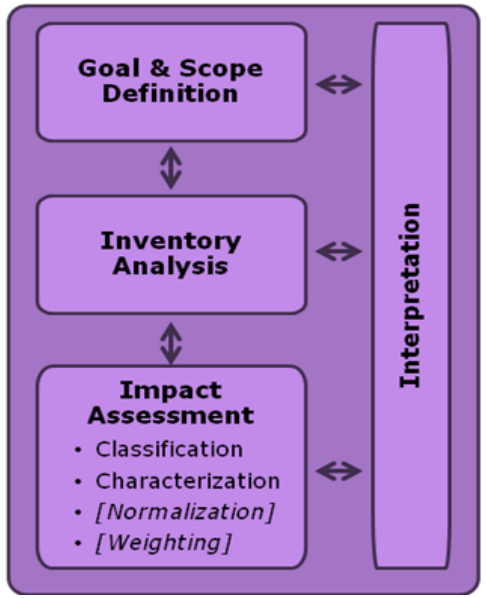

Stages of an LCA (ISO 14044)

The **objective** indicates the reasons for the study and the audience to whom the analysis is intended

The **scope** includes the definitions of the product system studied, the functional unit, the system boundary, the allocation procedures, the selected impact categories, the methodologies for assessing the impacts and their interpretation, the quality requirements of the data and assumptions underlying the analysis

The **life cycle inventory analysis** (LCI) implies the collection of the data necessary to achieve the objectives of the defined study

The purpose of the **life cycle impact assessment** (LCIA) is to provide additional information to help evaluate the LCI results of the product system in order to achieve a better understanding of their environmental significance.

Case Study

Functional unit (EN 14040): the reference quantity of a product system for which environmental impacts are calculated

20 cm thick base layer of 1 km length road asphalt pavement of a rural road (10 m wide) with an average annual daily traffic of 1500 vehicles per day

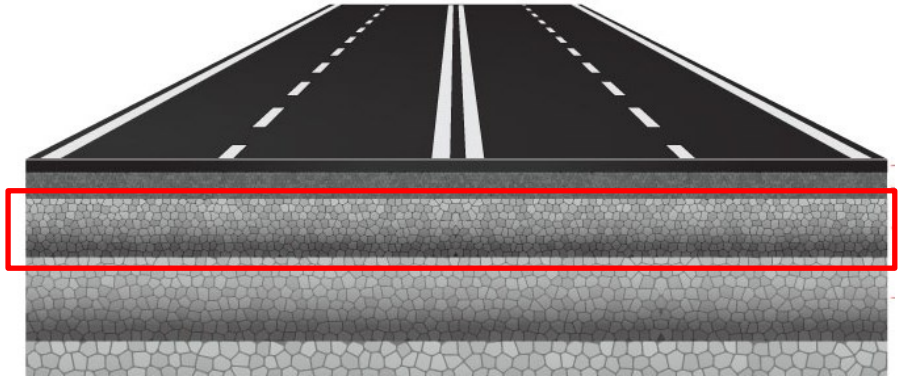

3 alternative functional units were the designed asphalt mixtures of a base layer made of **HMA**, **HMAJ** or **HMAJ+L**

Asphalt pavement design

Stress-strain state of an elastic homogeneous and isotropic multilayer subjected to ESAL load

Stiffness Modulus from laboratory investigation

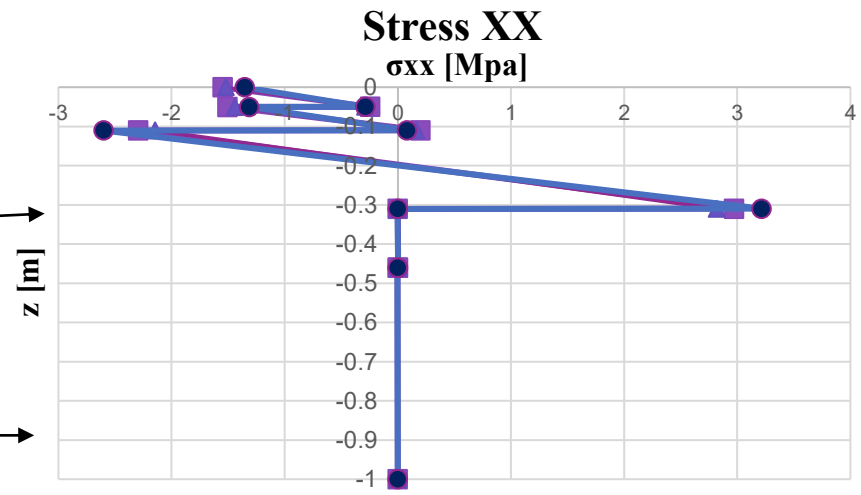

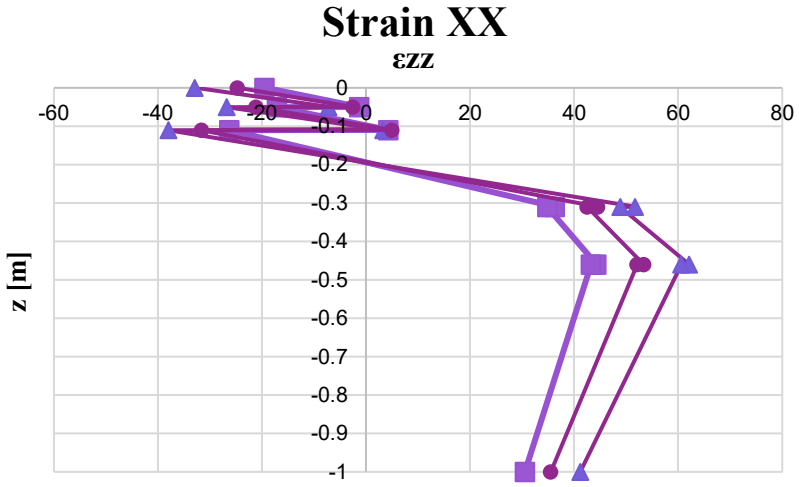

Case Study

Asphalt pavement design

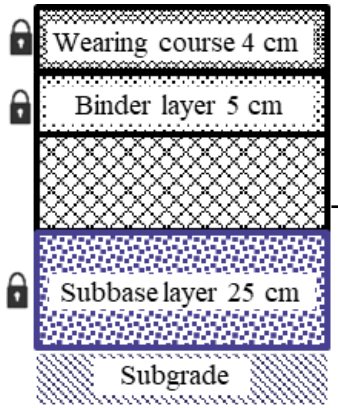

Base layer (20 cm)

- layout 1 with HMA as base layer has **16** years service life
- layout 2 with HMAL+J as base layer has **18** years service life
- layout 3 with HMAJ as base layer has **20** years service life

Service life predicted as the minimum number of ESALs that causes:

- fatigue cracking: FD<1 (Miner law)
- rutting: RD< 2 cm (Vaerstraten law)

The impact category indicators will be revised considering the number of years exceeding the service life of the reference pavement (Layout 1 with HMA as base layer)

$$I_{N,ij} = I_{ij} \cdot \left(1 - \frac{S_j - S_{LM}}{S_{LM}}\right)$$

Impact category indicator

Service life gap coefficient

LCA - unit processes

The system boundary of the present LCA follows EN 15804

HMA as base layer

UNI EN ISO 14040 – UNI EN ISO 14044

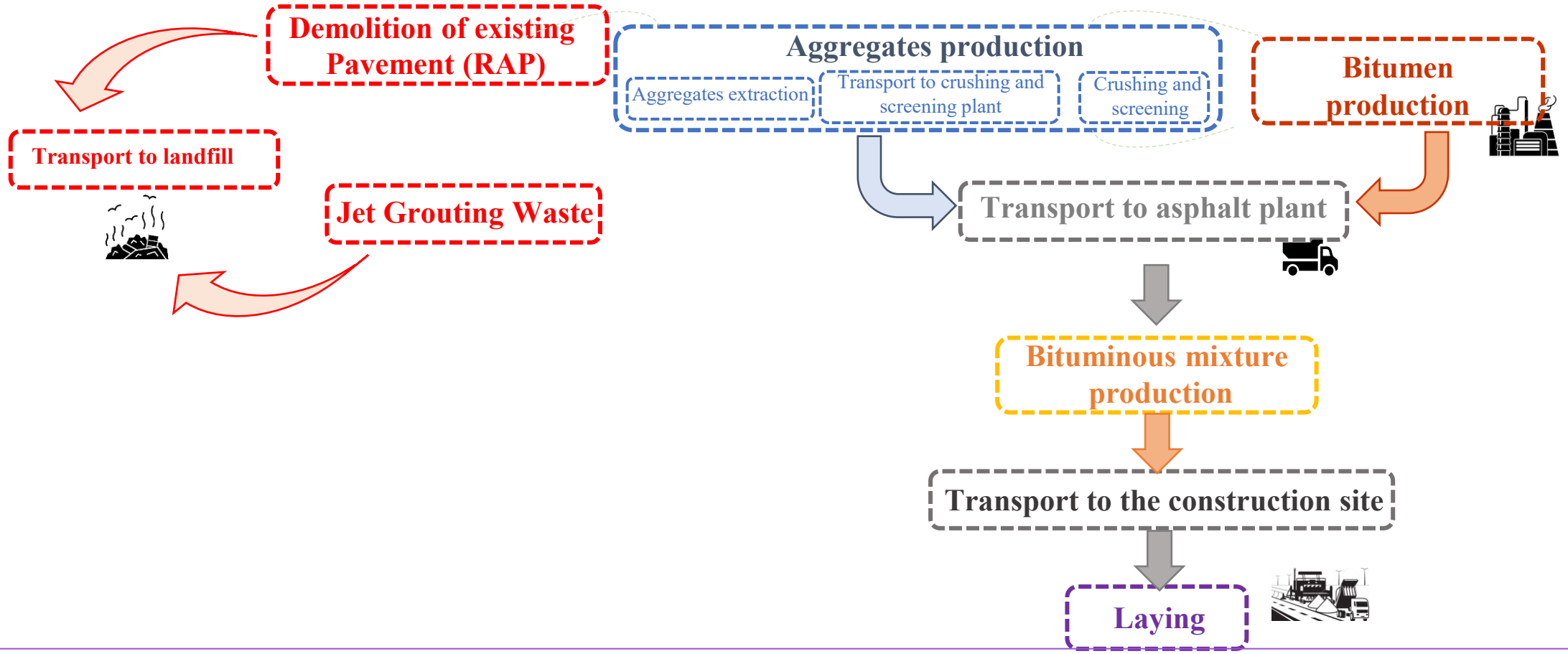

LCA - unit processes

The system boundary of the present LCA follows EN 15804

HMAJ as base layer

UNI EN ISO 14040 – UNI EN ISO 14044

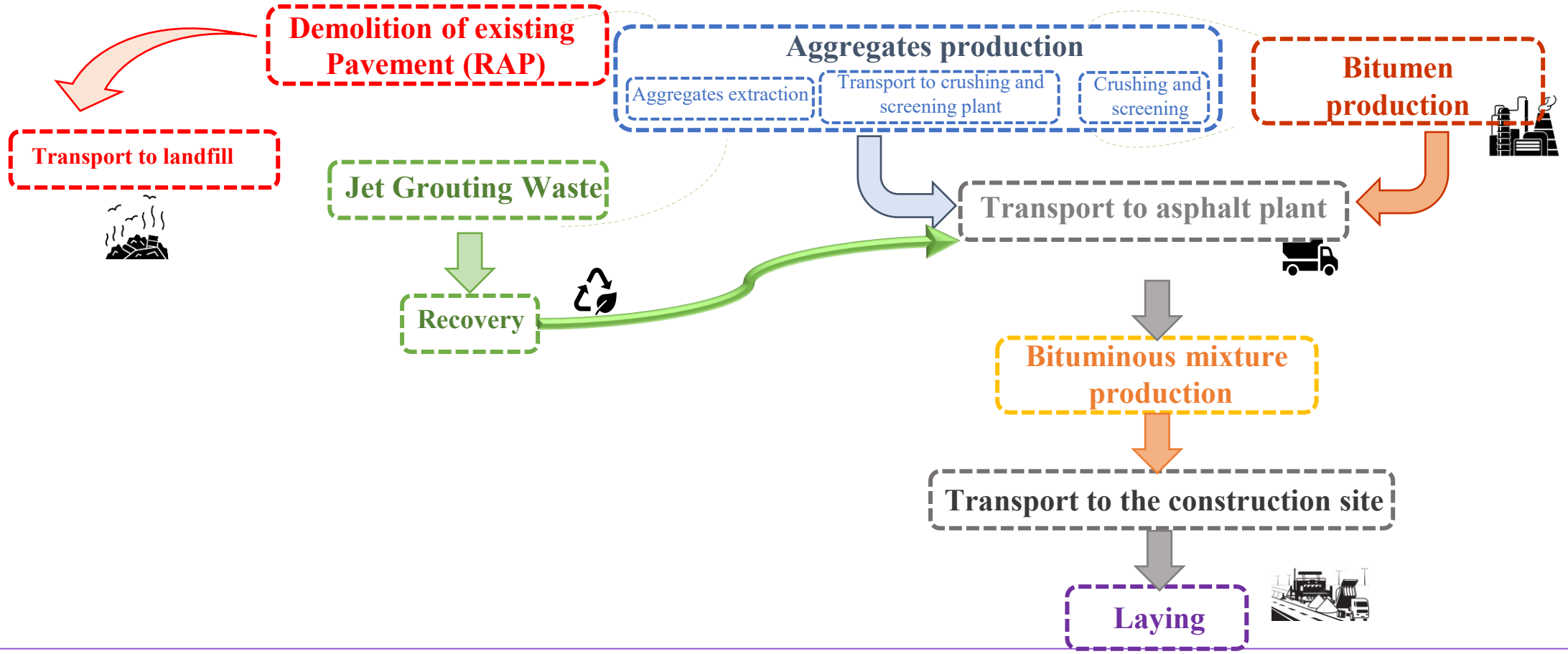

Life Cycle Inventory

Inventory and impact assessment phases were performed using SimaPro9® tool and the embedded databases (Ecoinvent 3, USLCI, Input Output database etc.)

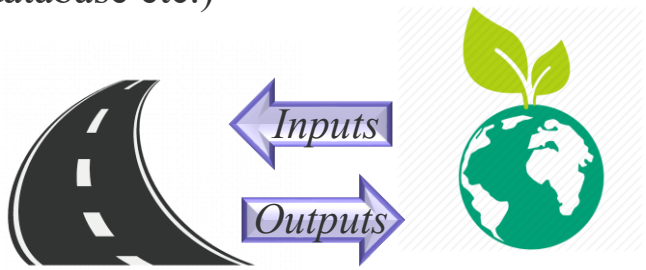

Primary data

- **Consumption of raw materials**, such as aggregates and bitumen
- **Distance traveled by trucks** for the transport of virgin materials, finished products and waste
- The number, type and characteristics of the **machinery** used for handling, putting in pear and demolition of materials

Secondary data

- **Fuel consumption** of trucks and construction equipment
- **Emissions** of volatile compounds and dust into the atmosphere due to the internal combustion of the engines of materials handling vehicles and to the combustion of natural gas and oil from industrial burners

Tertiary data

- Share of **electricity** produced with fossil and non-fossil fuels
- Data relating to the production of fossil fuels used in the various phases of the process

Life Cycle Assessment

LCA – Impact indicators

Global Warming Potential (GWP)		
Substance (Si)	**f_{GWP100}**	**Units**
CO_2	1	g CO_2/g Substance
CH_4	25	g CO_2/g Substance
N_2O	320	g CO_2/g Substance
CO	2	g CO_2/g Substance
IPA	3	g CO_2/g Substance

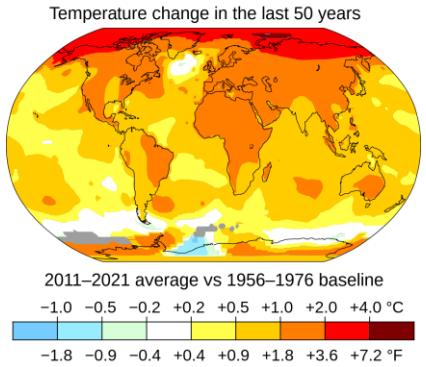

Acidification (AP)		
Substance	**f_{AP}**	**Units**
SO_x	1	g SO_2/g Substance
NO_x	0.7	g SO_2/g Substance
NH_3	1.88	g SO_2/g Substance

Photochemical Ozone Creation Potential (POCP)		
Substance	**f_{POCP}**	**Units**
CO	0.03	g C_2H_4/g Substance
VOC – Oil processing, Electricity production	0.50	g C_2H_4/g Substance
VOC – Diesel exhaust gases	0.6	g C_2H_4/g Substance

Eutrophication (EP)		
Substance	**f_{EP}**	**Units**
NO_x	0.3	g NO_3/g Substance
N_2O	0.64	g NO_3/g Substance
NH_3	0.82	g NO_3/g Substance

Total Suspended Particle (TSP)

Huibregts et al. (2016)

Life Cycle Assessment

LCA – Impact indicators

Materials consumption

Secondary raw materials (SRM)

Water

Bitumen

Aggregates

Waste production

Jet Grouting Waste

LCA Results

Category	Impact indicators	Units	HMA	HMAJ+L	HMAJ
Pollution	GWP	kg CO_2 eq. In 100 years	402527.83	400938.73	398103.50
	POCP	kg C_2H_4 eq.	342.56	311.93	295.34
	AP	kg SO_2 eq.	3077.51	3036.43	3021.96
	EP	kg NO_3 eq.	1109.62	1092.43	1088.03
	TSP	kg	243.13	229.80	212.65
Resource consumption	NRER	MJ	5324493.41	5120675.50	5032089.69
	Water	t	75.51	68.58	61.92
	Bitumen	t	527.26	513.64	500.43
	Aggregates	t	11678.43	11346.11	11029.10
	SRM	t	0.00	275.94	549.92
Waste Production	JW	t	549.92	273.47	0

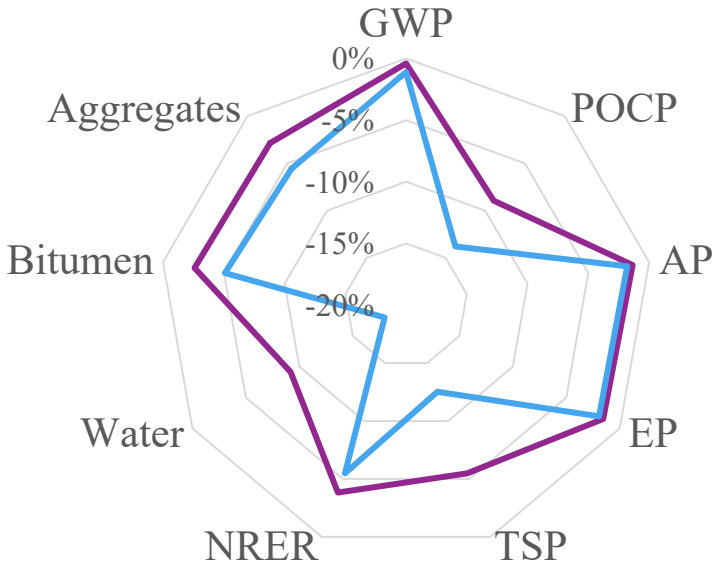

HMAJ vs HMA

-14% POCP **-12% TSP** **-18% Water consumption**

Multi-Criteria Decision Analysis

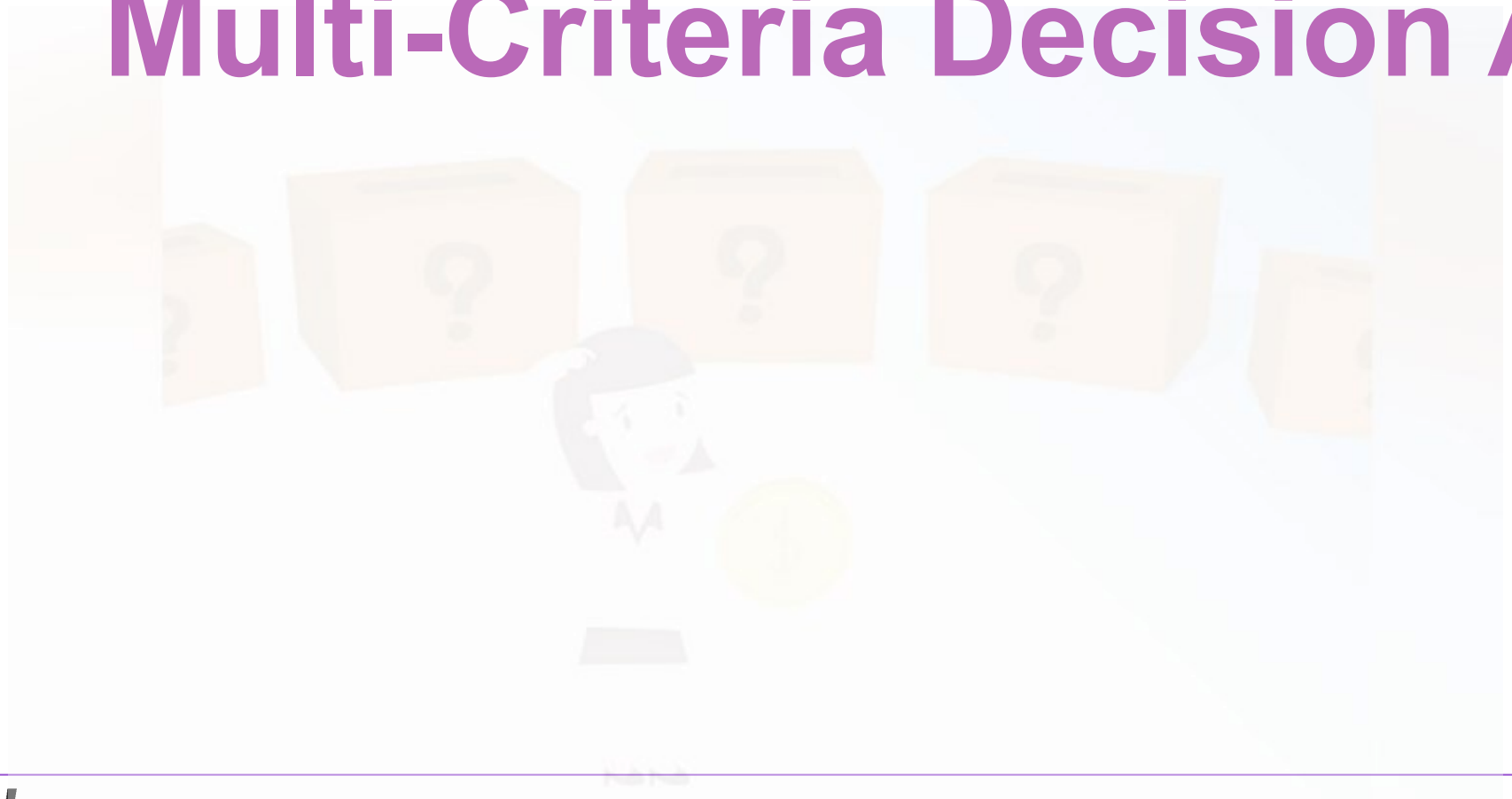

Multi-criteria decision analysis

Additional parameters were assessed

Investment costs

Cost items	Units	Layout 1 with HMA as base layer	Layout 2 with HMAJ as base layer	Layout 3 with CRA as base layer
Milling of existing bituminous layers until 3 cm depth	€	32147.51	32147.51	32147.51
Milling of the remaining depth of existing bituminous layers	€	67090.46	67090.46	67090.46
Transport to landfill within 10 km	€	30755.69	29750.47	1005.22
Transport to landfill beyond 10 km	€	81473.32	78810.44	2662.88
Charges of RAP disposal	€	41512.24	41512.32	41512.32
Charges of JW disposal	€	3146.40	1671.10	0
Laying of base layer	€	679198.08	665520.98	649520.98
Laying of binder layer	€	253154.29	253154.29	253154.29
Laying of wearing course	€	230140.26	230140.26	230140.26
Total	€	**1418618.25**	**1399797.83**	**1277233.92**

Technological complexity

Range	Attribute	Description
0	none	No additional equipment with respect to the traditional hot bituminous mixtures production and laying
0-0.25	low	Low influence of additional equipment on costs, on the number of construction equipment and on the skills needed by the workers
0.25-0.50	medium	Medium influence of additional equipment on costs, on the number of construction equipment and on the skills needed by the workers
0.50-0.75	high	High influence of additional equipment on costs, on the number of construction equipment and on the skills needed by the workers
0.75-1	very high	Very high influence of additional equipment on costs, on the number of construction equipment and on the skills needed by the workers

Laying time

Alternative pavements	JW recovery	Base layer laying	Wearing course + binder layer laying	Total
Layout 1	-	22 days	15 days	37 days
Layout 2	2 days	22 days	15 days	39 days
Layout 3	4 days	22 days	15 days	41 days

What is the most suitable alternative?

Multi-criteria decision analysis

The multi-criteria analysis methods support the decision maker in the organization and synthesis phase of complex and heterogeneous information

To support the MCDA to determine the robustness of evaluations by examining how much of the results can be influenced by changes in methods, models, values of unmeasured variables or hypotheses a **sensitivity analysis** was adopted

Decision matrix

Indicators	Units	Alternatives		
		Layout 1	Layout 2	Layout 3
GWP	kg CO_2 eq.	402527.83	400938.73	398103.50
POCP	kg C_2H_4 eq.	342.56	311.93	295.34
AP	kg SO_2 eq.	3077.51	3036.43	3021.96
EP	kg NO_3 eq.	1109.62	1092.43	1088.03
TSP	kg	243.13	229.80	212.65
NRER	MJ	5324493.41	5120675.50	5032089.69
Water	t	75.51	68.58	61.92
Bitumen	t	527.26	513.64	500.43
Aggregates	t	11678.43	11346.11	11029.10
SRM	t	0.00	275.94	549.92
Waste (JW)	t	549.92	273.47	0
Average Stiffness	MPa	3600	5000	5733
ITS	MPa	0.73	0.72	0.81
ΔITS	%	0.09	0.07	0.05
Fatigue damage	-	0.98	0.82	0.81
Rutting damage	cm	1.32	0.92	0.70
Investment costs	€	1418618.25	1399797.83	1277233.92
Laying time	days	37	39	41
Technological Complexity	-	0.00	0.55	0.65

Multi-criteria decision analysis

Since the aim of the research was to find a solution that can substitute a traditional solution in HMA, a new decision matrix was designed

Dimension of the criteria

Categories	Indicators	Units
Environmental	GWP	kg CO_2 eq. In 100 years
	POCP	kg C_2H_4 eq.
	AP	kg SO_2 eq.
	EP	kg NO_3 eq.
	TSP	kg
	NRER	MJ
	Water	t
	Bitumen	t
	Aggregates	t
	SRM	t
	RAP and JW	t
Mechanical	Stiffness	MPa
	ITS	MPa
	ΔITS	%
Durability	Fatigue damage	-
	Rutting damage	cm
Costs	Investment costs	€
	Laying time	days
	Technological Complexity	-

The **normalized** indicators were grouped into different categories and the normalized difference between each Layout from Layout 1 was calculated

New decision matrix

	Layout 1 vs	
Category	Layout 2	Layout 3
Environmental	6.21	11.00
Mechanical	1.05	2.89
Durability	1.59	2.00
Costs	-1.21	-1.00

Multi-criteria decision analysis

Sensitivity analysis

55 Weight vectors

Configuration	Weight vectors				
	1	2	3	4	5
0	0.250	0.500	0.167	0.167	0.167
	0.250	0.167	0.500	0.167	0.167
	0.250	0.167	0.167	0.500	0.167
	0.250	0.167	0.167	0.167	0.500
1	0	0	0	0	0
	0.333	0.333	0.600	0.200	0.200
	0.333	0.333	0.200	0.600	0.200
	0.333	0.333	0.200	0.200	0.600
2	0.333	0.600	0.333	0.200	0.200
	0	0	0	0	0
	0.333	0.200	0.333	0.600	0.200
	0.333	0.200	0.333	0.200	0.600
3	0.333	0.600	0.200	0.333	0.200
	0.333	0.200	0.600	0.333	0.200
	0	0	0	0	0
	0.333	0.200	0.200	0.333	0.600
4	0.333	0.600	0.200	0.200	0.333
	0.333	0.200	0.600	0.200	0.333
	0.333	0.200	0.200	0.600	0.333
	0	0	0	0	0
5	0	0	0	0	0
	0	0	0	0	0
	0.500	0.500	0.500	0.750	0.250
	0.500	0.500	0.500	0.250	0.750

Configuration	Weight vectors				
	1	2	3	4	5
6	0	0	0	0	0
	0.500	0.500	0.750	0.500	0.250
	0	0	0	0	0
	0.500	0.500	0.250	0.500	0.750
7	0	0	0	0	0
	0.500	0.500	0.750	0.250	0.500
	0.500	0.500	0.250	0.750	0.500
	0	0	0	0	0
8	0.500	0.750	0.500	0.500	0.250
	0	0	0	0	0
	0	0	0	0	0
	0.500	0.250	0.500	0.500	0.750
9	0.500	0.750	0.500	0.250	0.500
	0	0	0	0	0
	0.5	0.25	0.5	0.75	0.5
	0	0	0	0	0
10	0.500	0.750	0.250	0.500	0.500
	0.500	0.250	0.750	0.500	0.500
	0	0	0	0	0
	0	0	0	0	0

3 MCDA methods

ELECTRE

Concordance index

$$c_{kk'} = \sum_j w_j^* : X_{jk}^* > X_{jk'}^*$$

Discordance index

$$d_{kk'} = \max_j \{(X_{jk'}^* - X_{jk}^*) : X_{jk}^* < X_{jk'}^*\}$$

- w_j^* is the normalised weight value of the j-th indicator
- X_{jk}^* is the utility of j-th indicator of the k-th alternative
- $X_{jk'}^*$ is the utility of j-th indicator of the k'-th alternative

TOPSIS

Distance

$$\delta_k = \sqrt[q]{\sum_j w_j^* \cdot |X_{jk}^* - X_{jA^*}^*|^q}$$

- q is a coefficient $\in [1 \div +\infty]$, that identifies the type of distance calculated: i.e. q=1 Manhattan distance; q=2 Euclidean distance
- w_j^* is the normalized weight value of the j-th dimension
- $X_{jA^*}^*$ is the maximum utility of j-th dimension identified as ideal solution A^*

MULTY-UTILITY

Utility

$$U_k = \sum_j w_j^* \cdot X_{jk}^*$$

- w_j^* is the normalised weight value of the j-th indicator
- X_{jk}^* is the value of the j-th indicator belonging to k-th alternative

Multi-criteria decision analysis

Identification of the best suitable alternative

Frequency of appearance of the most suitable alternative considering Environmental, Mechanical, Durability and Cost criteria

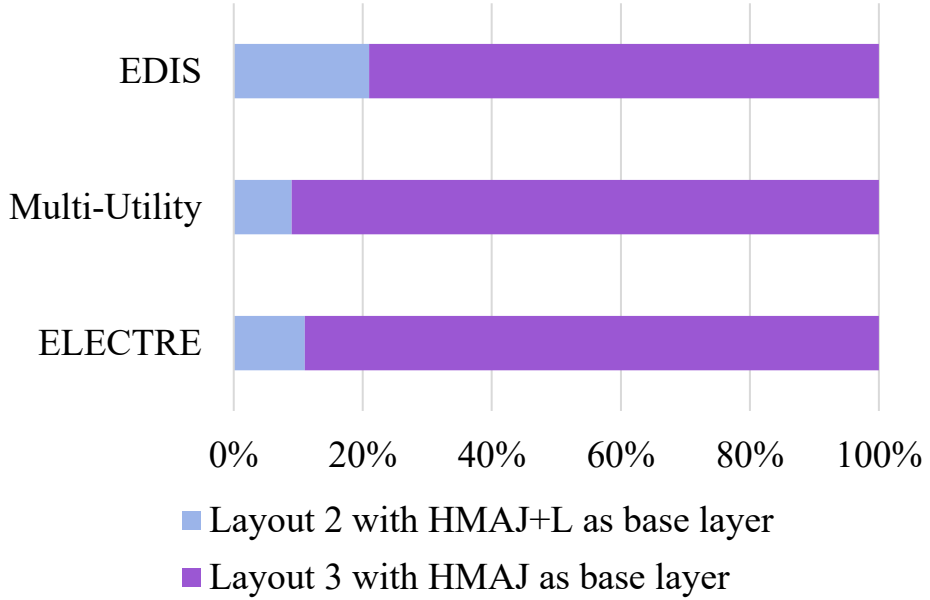

Layout 3

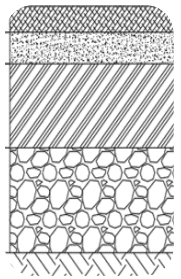

4 cm **Wearing course: HMA**
5 cm **Binder layer: HMA**
20 cm **Base layer: HMAJ**
25 cm **Subbase layer: granular mixture**

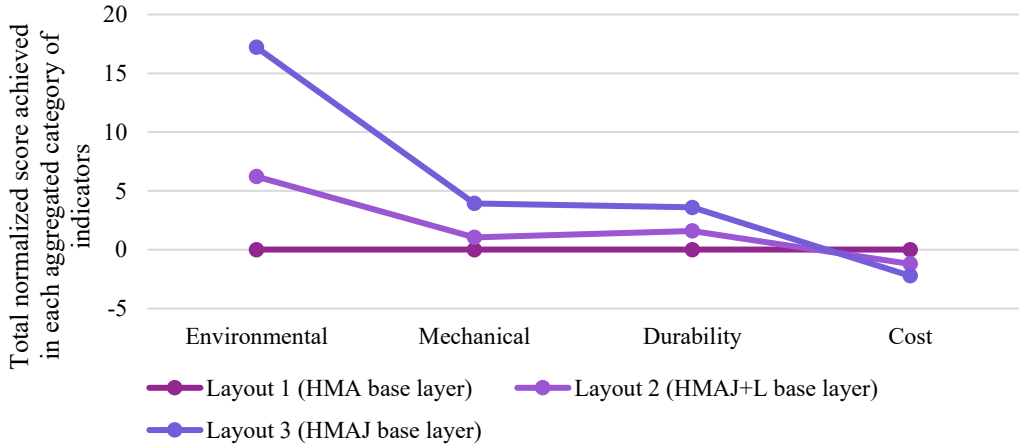

Conclusions

- From an environmental point of view the **LCA** results showed that, the more JGW is substituted to the limestone filler, the more the main impact category indicators decrease, shifting from -9% with up to -18% reduction for water consumption and from -3% up to -6% for non-renewable energy resources with either 2% JGW or 4% JGW substituted to the limestone filler
- The **multi-criteria decision analysis** results highlighted that, although the JGW recovery and reuse into hot asphalt mixture for the base layer increases the overall technological complexity and construction time of the maintenance intervention, the environmental and durability benefits make the HMAJ the most suitable alternative compared to both HMA and HMAJ+L
- The **sensitivity analysis** results confirm the robustness of the best alternative when varying the decision-making context, both in terms of weight vectors (55 configurations) and MCDA methods (3 methods)

5-9
SEPTEMBER
.22

Università di Napoli Parthenope

Prof. Ing. Francesca Russo
Università degli Studi di Napoli Federico II
Ing. Cristina Oreto
Università degli Studi di Napoli Federico II